Neural systems for memory-based value judgment and decision-making

Avinash R. Vaidya[1]
David Badre[1, 2]

[1]Department of Cognitive, Linguistic, and Psychological Sciences, [2]Carney Institute for Brain Science, Brown University, Providence, RI, 02912

ABBREVIATED TITLE: MEMORY-BASED VALUE JUDGMENT

Address correspondence to:
Avinash R. Vaidya
Brown University
Providence, RI 02912-1978
tel. 401-863-3634, fax 401-863-2255
email avinash_vaidya@brown.edu

Conflicts of interest: The authors declare no competing conflicts of interest.

Acknowledgements: This work was supported by a Multidisciplinary University Research Initiative award from the Office of Naval Research (N00014-16-1-2832), an award from the James S. McDonnell Foundation, and a Ruth L. Kirschstein National Research Service Award to A.V. (NIMH F32 MH116592-01A1). We are grateful to Michael Frank for helpful comments and suggestions on the manuscript, as well as Apoorva Bhandari and Andra Geana for constructive discussion on methods and analysis. Thanks also to Adriane Spiro for help with data collection, and Henry Jones for assistance with behavioral piloting and analysis of normative data.

Abstract

Real life choices often require that we draw inferences about the value of options based on structured, schematic knowledge about their utility for our current goals. Other times, value information may be retrieved directly from a specific prior experience with an option. In a functional magnetic resonance imaging experiment, we investigated the neural systems involved in retrieving and assessing information from different memory sources to support value-based choice. Participants completed a task in which items could be conferred positive or negative value based on schematic associations (i.e. schema value), or learned directly from experience via deterministic feedback (i.e. experienced value). We found that ventromedial prefrontal cortex (vmPFC) activity correlated with the influence of both experience- and schema-based values on participants' decisions. Connectivity between vmPFC and middle temporal cortex also tracked the inferred value of items based on schematic associations on the first presentation of ingredients, prior to any feedback. In contrast, the striatum responded to participants' willingness to bet on ingredients as a function of the unsigned strength of their memory for those options' values. These results argue that striatum and vmPFC play distinct roles in memory-based value judgment and decision-making. Specifically, the vmPFC assesses the value of options based on information inferred from schematic knowledge and retrieved from prior direct experience, while the striatum controls a decision to act on options based on memory strength.

Introduction

How can we predict the value of options without prior, explicit experience? For example, when building a table, a hammer has greater value than a ball of yarn. No previous experience using yarn in place of a hammer is needed to make this kind of value judgment. However, this evaluation does depend on knowledge about yarn, hammers and table construction. Structured knowledge about the world that can support this kind of inference is often referred to as a schema (Bartlett, 1932; Ghosh & Gilboa, 2014; Piaget, 1952). Judging the value of options for accomplishing complex goals, like table building, requires inference based on these schematic representations.

Value does not always need to be inferred. In the same example, seeing a certain brand of varnish on display might remind you that your friend had recommended that varnish for your table last week. In this case, value relies on the retrieval of an explicit positive association with the item from a specific time and place. Here, value is a memorized feature of one or a few previous episodes, which may be brought to mind through mechanisms of episodic retrieval.

Relatively little is known about the neural systems involved in retrieving information from different memory sources to support value judgment. Lesion studies have shown that ventromedial prefrontal cortex (vmPFC) and orbitofrontal cortex (OFC) are necessary for decision-making when option values must be inferred from knowledge of task structure, but not when values can be retrieved from directly learned associations (Bradfield, Dezfouli, van Holstein, Chieng, & Balleine, 2015; Izquierdo, Suda, & Murray, 2004; Jones et al., 2012; Reber et al., 2017). It is unclear if these deficits arise because these regions represent task structure (Schuck, Cai, Wilson, & Niv, 2016; Wilson, Takahashi, Schoenbaum, & Niv, 2014), guide

retrieval based on these schemas (Eichenbaum, 2017), or specially utilize structured knowledge during value judgment.

A parallel line of research has focused on the striatum at the intersection of goal-directed retrieval and value-based decision-making. Recent work has argued that the striatum is involved in assessing the value of information stored in memory and using this information to bias cortical representations of choices with higher value (Shadlen & Shohamy, 2016). A mutually compatible alternative is that striatum integrates memory signals into its basic decision making functions, including those related to memory itself (Han, Huettel, Raposo, Adcock, & Dobbins, 2010; Scimeca & Badre, 2012), though these may also be separable processes (Elward, Vilberg, & Rugg, 2015).

The function of these regions in value judgment likely further depends on coordination with several other regions for the retrieval of relevant information. Notably, overlapping regions within the vmPFC and the striatum are connected with regions canonically associated with episodic and schematic memory, and adaptive retrieval, including the hippocampus (HPC), middle temporal cortex (MTC) and anterior ventrolateral prefrontal cortex (aVLPFC) (Haber & Knutson, 2010; Price, 2007). However, it is not known how these regions interact to link retrieval to decision-making.

We tested three hypotheses from this prior literature on memory and value-based decision making using a functional magnetic resonance imaging (fMRI) experiment: (1) vmPFC is preferentially engaged when value judgments are based on structured knowledge about the world (i.e. schema memory). (2) Striatum tracks directly experienced (rather than inferred) values. (3) vmPFC and striatum interact with different memory stores in accord

with their respective roles in constructing values through schema-based inference (vmPFC) versus direct, explicit experience (striatum).

Our results were inconsistent with these *a priori* hypotheses, but yielded new insights into the brain systems linking memory with value-based decision-making. Striatum responded to the effect of the unfamiliarity of options on participants' value judgments, not the value of the options themselves. On the other hand, vmPFC responded to the influence of both the experienced and schema-based value information on value judgments. Analysis of connectivity between these regions and memory stores revealed greater communication between the striatum and HPC in response to demands on recall of experienced values, while vmPFC and MTC communication increased in response to inferred schema-based values. Thus, vmPFC represented retrieved value information from multiple memory sources, and coordinated with MTC when value was inferred. In contrast, the striatum incorporated basic memory strength into the decision process, and increased communication with HPC in response to demand for retrieval of experienced values. These results advance a new understanding of memory-based value judgements and outline distinct roles for these regions.

Methods

Behavioral Task and Experimental design

We investigated the neural systems involved in making value judgments based on different memory sources using a novel experimental task. This task, and all other tasks not administered through Amazon Mechanical Turk (AMT), were programmed in Psychtoolbox-3 (Brainard, 1997; Kleiner, Brainard, & Pelli, 2007). In this experiment, participants took the role of a restaurant chef choosing whether or not to serve ingredients to a customer (Figure

1). Each trial required participants to make a bet based on their belief that the customer would like or dislike the displayed ingredient. Participants were instructed that if they served an ingredient that the customer liked, they would receive 50 points, however if they served an ingredient that the customer did not like, they would lose 25 points. If participants chose not to serve an ingredient, they would receive 0 points.

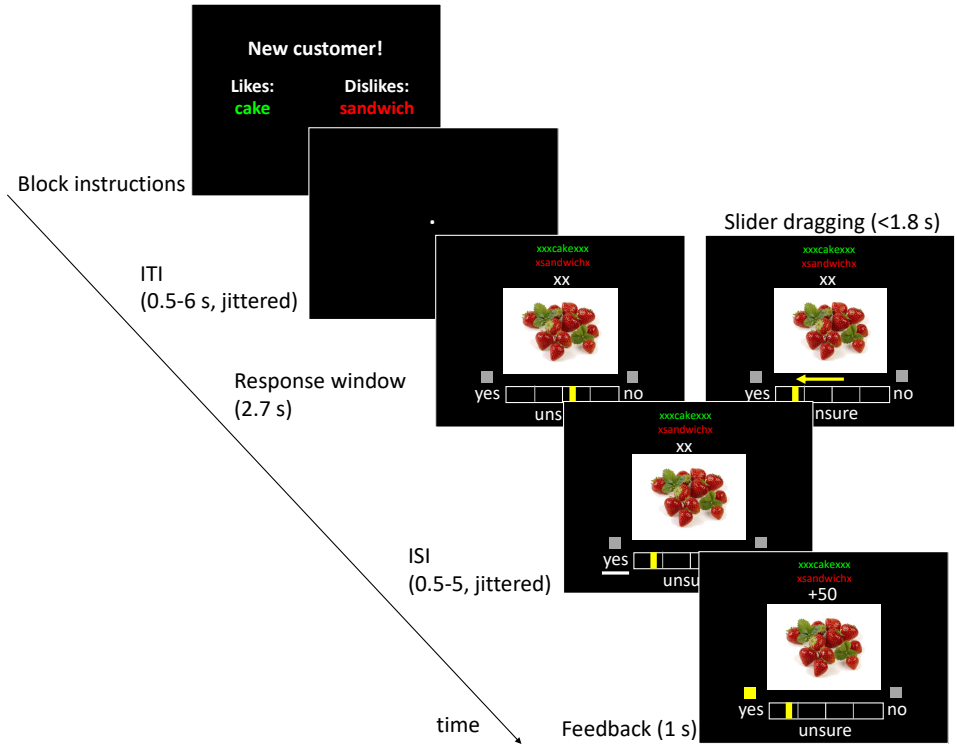

Figure 1. Task schematic showing instructions at the start of a block and organization of a single example trial. At the start of the block, participants were informed of the recipes that customer liked and disliked. These recipe names were presented in green and red above the ingredient on all trials. In each trial, participants indicated their decision to feed the displayed ingredient to the current customer, and their confidence in this decision, using a slider. Participants then saw whether or not the customer liked the ingredient, signaled by a box above either response cue, and the points earned or lost in each trial. ITI (inter-trial interval), ISI (inter-stimulus interval).

After the participant made their choice, the customer's preference for a given ingredient was always signaled by a cue above the correct response during feedback, regardless of whether the participant chose to feed the customer or not, and all customer preferences were deterministic. Thus, participants received complete information on each

trial regardless of their response. The feedback provided a source for learning the value of an individual ingredient. If the participant did not respond in time, no information about the customer's preferences was given and participants were shown the word 'slow' in place of feedback about points earned.

In addition to the information about ingredient preferences provided through feedback, participants were told at the start of a block that the customer liked ingredients pertaining to one recipe (positive recipe) and disliked another (negative recipe). In this way, the participant could also infer the value of an ingredient on the basis of schematic knowledge about what ingredients go with what recipes, without having received feedback. For example, if the customer liked cake and disliked soup, flour might be positively valued and onions might be negative by virtue of their association with each recipe.

At the start of each block, participants were told that they were about to feed a new customer, and were given the names of the recipes that the customer liked and disliked. The two recipes in each block were randomly selected without replacement from a set of six recipes. The screen was then left blank for 12 s until the start of the first trial.

Participants were also instructed before the start of the task that each customer liked and disliked other ingredients that were unrelated to these recipes (i.e. 'independent ingredients'). The value related to these ingredients could not be anticipated in advance based on their schematic associations, but rather would have to be acquired through experience.

Each ingredient was repeated three times throughout a block. For these repeated ingredients, participants could retrieve a memory of previous feedback to make a decision.

All repetitions were separated by at least one other ingredient so that participants were never making decisions about the same ingredient for multiple trials successively.

Thus, the experiment had three factors by design: ingredient clustering (recipe or independent), value (positive or negative) and presentation number (1, 2, 3). For the purposes of behavioral and fMRI analysis, any missed responses were not considered in the count of ingredient presentations, as no value information was communicated to the participant on these trials (e.g. if a participant missed the response deadline on the first presentation, the second presentation would be considered the first, and the third presentation would be considered the second in all analyses).

In each trial, participants saw an ingredient and were asked to respond by moving a slider to either side of a bar to indicate their decision to serve an ingredient and their confidence in that decision with a single response, similar to Scimeca, Katzman, and Badre (2016). Moving the slider past the midway point to either side was considered a binary selection of that side's response, while the distance of the slider from the midway point provided a continuous index of confidence. The slider would start in a random position on each trial and participants could then drag it toward the left or the right by holding down a button on a fiber optic response pad (Current Designs, Philadelphia, PA) using their right index or middle fingers. The slider would stop moving when it reached an end of the bar, or when participants let the button go. Participants could not change the slider position after letting go of the button. The side of bar where participants placed the slider signaled their choice, and the distance of the from the middle of the bar indicated their confidence.

Before the fMRI experiment, participants completed a practice task in which they learned to use the slider while verifying various general knowledge statements (e.g., 'Black

174 bears are omnivores'), and indicate their confidence in their response. Participants received
175 further practice outside the scanner by completing a short practice block of the restaurant
176 task where they fed a customer with recipes and ingredients that did not appear in the fMRI
177 experiment.

178 Trials were preceded by a jittered inter-trial interval (ITI) drawn from a lognormal
179 distribution (0.5-6 s). In each trial, participants saw a food ingredient centrally displayed for
180 up to 2.7 s, during which time they could choose whether or not to feed the ingredient to the
181 customer ('yes'/'no'). The names of the recipes that each customer liked and disliked
182 appeared at the top of the screen on each trial, color coded to indicate the customer's
183 preference.

184 After a response, there was a jittered inter-stimulus interval (ISI) drawn from a
185 uniform distribution (0.5-5.5 s). The remaining time from the response window and slider
186 movement period was also added to this interval. Participants then saw feedback about their
187 decision for 1 s. A square above the correct answer would light up, and the amount of points
188 added or subtracted from participants' total would be displayed in this period.

189 Trial-order, ITI and ISI lengths were drawn from sequences optimized for efficient
190 estimation of the hemodynamic response across conditions of interest. These sequences
191 were optimized by generating 5000 random sequences, and using SPM12 to create event-
192 based design matrices for stimuli and feedback events in each sequence. The average
193 variance for each regressor explained by all other regressors in the matrix was calculated for
194 each sequence and multiplied by the total duration of the sequence to approximate design
195 efficiency. The three sequences with the lowest values in this measure (i.e. least covariance

196 in regressors with the shortest experiment time) were used for the fMRI experiment and
197 were randomly ordered for each subject.

198 *Participants*

199 Twenty-six participants were recruited from the Providence, RI area to participate in
200 the fMRI experiment. Two participants were excluded due to movement greater than our
201 voxel size on at least one dimension during the functional scan, and one was excluded for
202 falling asleep during the experiment. Of the remaining 23 participants, four were male, their
203 mean age was 22.5 years (SD = 4.0), and their mean years of education was 15.5 (SD = 2.3).
204 All participants were right-handed, had normal or corrected-to-normal vision, and were
205 screened for the presence of psychiatric or neurological conditions, psychoactive medication
206 use, and contraindications for MRI. Two participants rejected all ingredients on the first
207 presentation of the positive independent condition, prohibiting analysis of their behavior or
208 ROI-level responses in a full 12-condition ANOVA after filtering for correct responses. One
209 participant did not commit any errors on the second or third presentation of the positive
210 recipe ingredients, prohibiting analysis of their error trials in this condition.

211 Two hundred participants from the United States were recruited through Amazon
212 Mechanical Turk (AMT) to provide normative naming responses for images of food
213 ingredients. Four of these subjects were rejected for exceptionally low accuracy in this task
214 (> 50%). The mean age of the remaining participants was 35.4 years (SD = 10.5), and 107 of
215 them were male.

216 A second sample of 221 participants were recruited from the United States through
217 AMT to provide normative data for ingredient-recipe associations. Twenty-nine of these
218 participants were rejected for failing to follow task instructions (most often by simply

writing the names of the ingredients rather than associated recipes). The remaining participants had a mean age of 36.0 years (SD = 11.1), and 71 of them were male.

All participants across experimental and norming studies gave informed consent as approved by the Human Research Protections Office at Brown University, and were compensated for their participation. Participants in the fMRI experiment also received a monetary bonus proportional to the points they earned in the main task.

Stimuli

Ingredient stimuli were obtained from the bank of standardized stimuli (BOSS; N = 65) (Brodeur, Dionne-Dostie, Montreuil, & Lepage, 2010; Brodeur, Guerard, & Bouras, 2014), food-pics database (N = 50) (Blechert, Meule, Busch, & Ohla, 2014), with a small set of supplemental food images collected by A.V. from Google Images (N = 4). These images were selected to include basic food ingredients — i.e. items that might be used as parts of a recipe, rather than completed meals. For example, an image of cheese would be included rather than an image of a pizza. All images were scaled to the same size and padded with white pixels or cropped to fit the same area. Ingredients from the BOSS database were excluded if more than 20% of the normative sample either responded that they did not know the name of the ingredient or did not recognize the ingredient. Ingredients were also rejected if the modal name for the ingredient given by respondents was incorrect (indicating low recognition accuracy), and if the H-value (a measure of naming disagreement across participants, similar to entropy) was above 3.00.

Because similar naming data were not available for ingredients from food-pics or Google Images, normative naming data were obtained through an AMT experiment. Participants were shown ingredient images and asked to write the name of the ingredient in

a text box below, or write "I don't know." Responses that included common variants of ingredient names were considered correct, while overly general names were marked as incorrect (e.g. 'nuts' for an image of pecans). Ingredients where more than 20% of participants did not know the name, or gave incorrect answers, were rejected. Naming agreement was also examined by calculating an H-value for each ingredient; however, this value did not exceed 3.00 for any ingredient in this set.

Normative recipe associations

Associations between ingredients and recipes were obtained through a norming experiment conducted on AMT akin to single word generation paradigms used to derive word associations (Postman & Keppel, 1970). Participants were shown ingredient images one at a time and were asked to write the name of the first recipe that came to mind using the ingredient shown on screen. Unique recipe names were then extracted for each ingredient and two researchers (A.V. and H.J.) manually processed these data. Alternative names, semantically similar responses and misspellings were all collapsed into single recipes, and ingredient specific information was removed to facilitate detection of overlap in ingredient-recipe associations (e.g. responses like 'pumpkin soup' and 'mushroom soup' were both reclassified as 'soup'). The end result of this process was a matrix with endorsement counts for 102 ingredients in 1876 recipes. Six ingredients were then dropped from this set, as they were visually too similar to other ingredients in the experiment, leaving 96 ingredients total.

Of these recipes, many (915) were only named by a single AMT participant for a single ingredient. As our task design required that each recipe have a large number of associate ingredients (at least seven recipe ingredients, and some additional ingredients to be used as

independent items), we cycled through different parameters for filtering out recipes. With each of these filtered lists, ingredients were assigned to hierarchically organized clusters using the Matlab (Mathworks, Natick, MA) function 'linkage,' which sorted ingredients based on the mean cosine similarity of their naming frequencies. Through this process we selected six recipes where the clustering solution provided ingredient cluster sizes that were large enough for our task design (pasta (N=10), soup (N=13), cake (N=15), pie (N=21), salad (N=17) and sandwich (N=20)).

Value rating task

At the start of the experimental session, participants completed a short rating task where they were asked to provide ratings for how much they would hypothetically want to have each ingredient at the end of the session. Participants provided responses on a seven point Likert scale from -3 to 3, with labels on -3 reading 'Not at all,' 0 reading 'Indifferent' and 3 reading 'Very much.' These subjective value ratings were included as a nuisance variable in each of the parametric GLM analyses. This task also served to visually familiarize participants with all ingredient images.

Computational modelling of behavior

Computational models of behavior were used to characterize the dynamics underlying participants' behavior in this task. We developed a simple base model that made a set of assumptions about behavior in this task that were carried over to all alternative models. Each alternative model made a modification of this base model, or the best model from the last step. Alternative models were compared based on their improvement in AIC scores from the last best fitting model from a previous step. For simplicity, below we present the final best fitting model that resulted from this process. We also briefly describe

alternative model modifications that did not survive the selection process in the following section.

Within the best fitting model, the value (*V)* of the ingredient (*i)* on each trial was calculated as:

$$V_i = \beta_0 + \beta_u(1 - |EV_i|) + \beta_e EV_i + \beta_s SV_i \text{ (Eq. 1)}$$

Where β_e controls the influence of experienced values (EV), and β_s controls the influence of schema values (SV) for the current trial ingredient (these two terms were included in the base model). The parameter β_u is a free temperature parameter that could be positive or negative and controls the model's tendency to endorse or reject an ingredient based on its unfamiliarity (the opposite of the absolute value of the experienced value term — described below; unfamiliarity model). An intercept term, β_0 captures overall, item-independent biases toward betting or passing (fixed bias). The model's willingness to bet on each trial (i.e. the model-P(yes)) was then calculated by placing V_i in a simple logistic function.

On each trial where participants responded, the experienced value for each ingredient was updated according to a simple Rescorla-Wagner learning rule (Rescorla & Wagner, 1972):

$$EV_i = EV_i + \alpha(outcome - EV_i) \text{ (Eq. 2)}$$

Where the value for *outcome* could be 1 or -1, depending on whether the feedback was positive or negative. While this rule is more commonly used in the context of reinforcement learning, it was adopted here as a simple means of operationalizing a graded memory that is signed and becomes stronger with repetitions of consistent value associations. The parameter α was a fixed learning rate that was fit for each subject in an alternate version of the base model where β_e was held at different constant values (1, 2, 5 and 8). The model fit

with a constant value of 5 for β_e had the lowest average negative log-likelihood of constants tested, and so α values from this fit were used in the base model and all further variations. This procedure to separately fit α was followed because β_e and α could not be stably estimated within the same model. Estimating these parameters separately allowed us to roughly capture individual differences in the encoding of *EV,* while separately estimating the contribution of *EV* to choice behavior through β_e. Allowing α to vary was also found to reduce the AIC of the base model over a variant where α was fixed to 1.0.

To reflect forgetting, the values for all ingredients also decayed towards zero with each trial according to:

$$EV_{t+1} = EV_t - dEV_t \text{ (Eq. 3)}$$

Where *d* is a parameter that controls the rate of this decay (also included in the base model).

Schema values were calculated through a weighted difference of the associative strength of ingredients with positive and negative recipes. The associative strength of each ingredient with these recipes was determined through a procedure based on latent semantic analysis (LSA) (Dumais, 2004; Landauer et al., 1998). The endorsement frequencies for ingredients across all recipes in the normative AMT data were weighted by their entropy across recipes and a singular value decomposition (SVD) was carried out on this matrix. This matrix was then reconstituted with a smaller number of dimensions set by a free parameter *c* (dimensions model). This parameter essentially controlled the dimensionality of recipe space that the model would consider, so that a lower dimensional model would separate ingredients on only simple features (i.e. savory or sweet), while a higher dimensional model would include increasingly granular information that separates ingredients along information about specific recipes (Figure 2). The association of an ingredient with each

recipe was calculated as the mean cosine similarity between that ingredient and all ingredients in each recipe cluster within this reconstituted matrix.

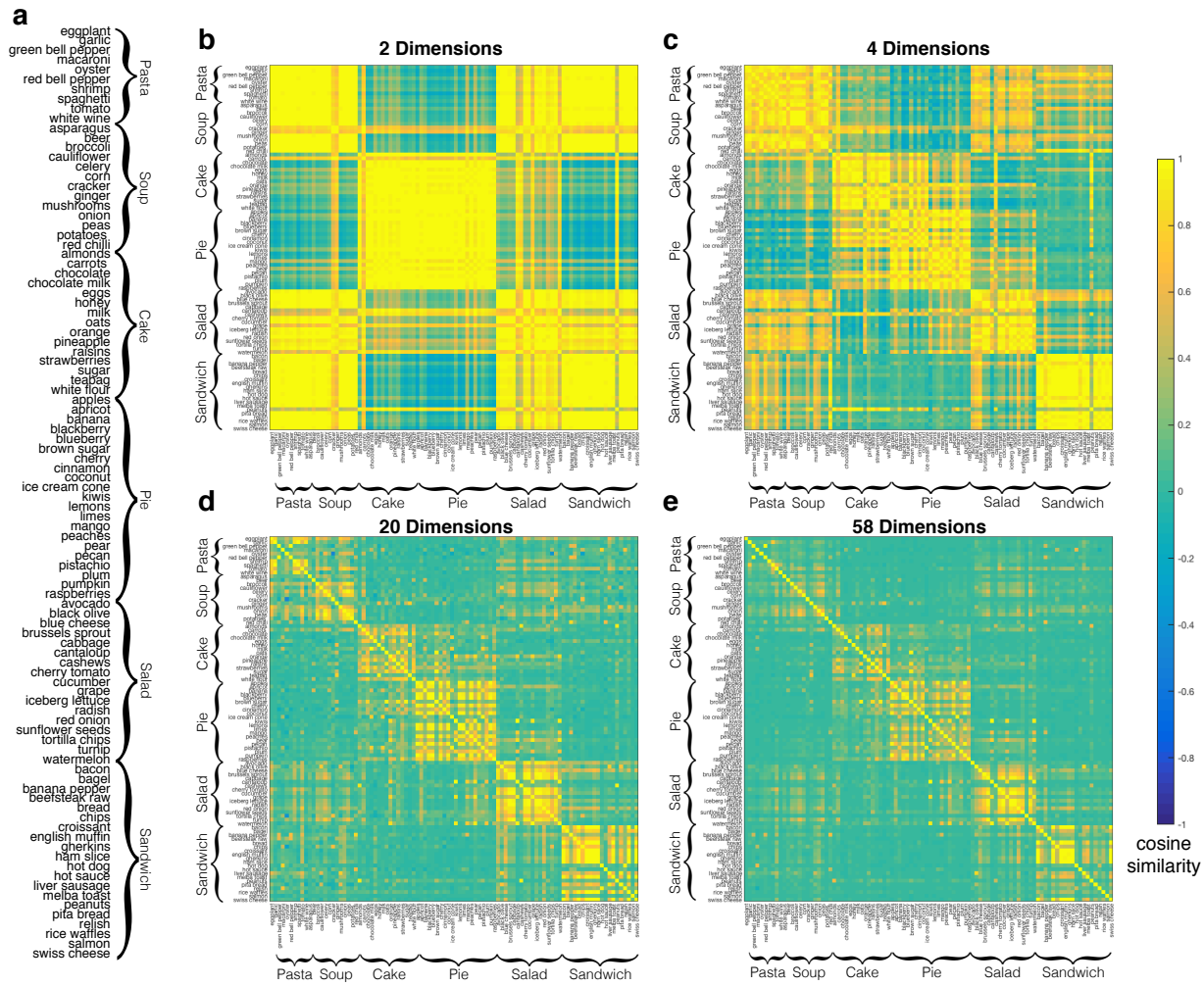

Figure 2. Example ingredient by ingredient cosine similarity matrices from reconstructions of ingredient-recipe associations with increasing dimensions. **a.** Ingredient names and clustering by recipe. **b.** Cosine similarity matrix with two dimensions **c.** with four dimensions, **d.** with 20 dimensions, and **e.** with 58 dimensions.

The recipes in a block could vary in their similarity, making some ingredients plausibly associated with both positive or negative recipes (e.g. pie and cake). To accommodate this possibility, the associative strength of ingredients with the positive and negative schemas to the schema was weighted by an estimate of participants' uncertainty

about the recipe associations of each ingredient, calculated as the probability that an ingredient was associated with both recipes (schema similarity model; $P(SR)$):

$$P(SR)_i = \frac{1}{1+\exp\left(-\beta_{sim}\left(1-\frac{|PR_i-NR_i|}{RRD}\right)\right)} \text{ (Eq. 4)}$$

Where RRD corresponds to the range of recipe association differences (i.e. the difference between the maximum and minimum recipe associative strength for all ingredients and recipes). This probability was then used in calculating weights for the sum and difference of the positive and negative recipe associations, where the weight for the sum of these associations was calculated as

$$w_{same} = 2(\,P(SR)_i - 0.5) \text{ (Eq. 5)}$$

And the weight for the difference of these ingredient associations was calculated as

$$w_{diff} = 1 - 2\,|P(SR)_i - 0.5| \text{ (Eq. 6)}$$

SV was then calculated as the weighted combination of the difference and sum of each ingredient's associative strength with the positive and negative recipes:

$$SV_i = w_{same}\,(PR_i + NR_i) + w_{diff}\,(PR_i - NR_i) \text{ (Eq. 7)}$$

The parameter β_{sim} controlled sensitivity to the similarity of ingredients' recipe associations, and the relative contribution of the difference or sum of positive and recipe associations to SV. This parameter also controlled the valence of the additive strength of these associations: positive or negative values for β_{sim} would give the same valence to the additive strength of recipe associations, respectively. Alternatively, if the β_{sim} parameter was zero, participants would rely solely on the difference of the ingredient's associative strength with the positive and negative recipes.

Alternate model parameters

Briefly, the following alternate modifications to the base model were considered, but did not improve model fitness:

(1) Asymmetric schemas model

This model included separate temperature parameters for positive and negative schema values, so that the value of an ingredient was:

$$V_i = \beta_e EV_i + \beta_{sp} PR_i - \beta_{sn} NR_i \text{ (Eq. 4)}$$

Where β_{sp} and β_{sn} are temperature parameters that control the influence of ingredient associations with positive and negative recipes, respectively.

(2) Schema discounting model

As participants learned the deterministic values of ingredients from feedback, it might be useful to use schema information less. This model assumed that when ingredients were associated with greater memory strength for the experienced values (i.e. the absolute value of EV), the schema value information would be exponentially discounted. Such a process might take place if participants traded off in retrieving information from different memory sources, especially when one is more reliable. For each ingredient, a discount factor was calculated as:

$$discount = \exp(-k|EV_i|) \text{ (Eq. 10)}$$

Where k was a free parameter that determined the steepness of this discounting. This discount factor was then included in the calculation of ingredient values:

$$V_i = \beta_e EV_i + discount\ \beta_s SV_i \text{ (Eq. 11)}$$

So that the contribution of schema values scaled with this exponential discounting factor.

(3) Dual Process Recollection Model

While the above models assume that experienced values are stored in episodic memory via a graded process, other models developed in memory judgment tasks suggest that episodic memory has a graded component (familiarity) and a discrete component (recollection) (Yonelinas, 1994). To test whether experienced values in this task may also rely on an additional non-graded recollection process, ingredient values were calculated as:

$$V_i = \beta_e((1 - P_r)EV_i + P_r RV_i) + \beta_s SV_i \text{ (Eq. 12)}$$

Where RV is the recollected value of an ingredient, i.e. the outcome from previous trials that does not decay or change over time (-1 or 1), and P_r is a fixed probability of recollection that does not change over trials. Thus, in this model, values learned through feedback contributed to the decision as the sum of recalled and graded value information, weighted by the probability of recall.

Model fitting and comparison

Participants' responses consisted of two main features: a binary response indicating whether or not to feed an ingredient to a customer, and a continuous rating of their confidence in this binary response. This confidence response could also be transformed into a continuous measure of participants' belief that a customer would like an ingredient (i.e. P(yes)) by measuring the position of the slider between the 'yes' and 'no' options rather than the distance of the slider from the middle, similar to Scimeca et al. (2016). Models were fit to both participants' continuous and binary choice responses. The overall model likelihood was calculated as the product of the model likelihood for participants' binary responses, and the model likelihood of the linear fit between the logit transformed model-P(yes) and participant-P(yes). The negative log of this likelihood function served as the objective

function to be minimized in the fitting procedure carried out by the Matlab function 'fmincon.'

Computational models were fit to participants' behavior in a step-wise process. At each step, a simpler preferred model was modified by the addition of new free parameters and the Akaike Information Criterion (AIC) of the simpler model and modified models were compared with a one-tailed t-test, as the addition of these new parameters was predicted to reduce AIC. The model with the best improvement in model fitness across subjects (i.e. the largest t-statistic in this comparison) was then considered the preferred model in the next step. Additional parameters that significantly reduced AIC were added to the preferred model and compared in the next step ($P < 0.05$). The search for the best fitting model was stopped once additional parameters no longer significantly improved model fitness, or when the parameters to search across were exhausted.

Each model was fit separately for each subject 20 times with randomized starting positions. The set of parameters with the lowest negative log-likelihood from each set of fits was saved and the other parameter fits were discarded. These 20 separate fits helped guard against the influence of idiosyncratic differences in starting point on the recovered parameters, and the possibility that the model fitting process would converge on local minima in the negative log-likelihood function.

Parameter recovery test

To verify that all parameters of the best fitting model could be recovered, we generated 100 simulated datasets with randomized parameters. The parameter d was generated from a uniform distribution from 0 to 0.05. Parameters β_e and β_s were generated from a lognormal distribution with a mean of 5 and standard deviation of 0.5. Parameters

β_0, β_m and β_{sim} were all generated from a standard normal distribution (mean 0, standard deviation of 1). The c parameter was generated from a uniform distribution ranging from 2 to 58. Given that these parameters were randomly generated and did not share the covariance of the real parameters fit to participants' behavior, this test could overestimate their recoverability. Thus, we further verified the recoverability of these parameters by fitting the model to data simulated using the parameters fit to participants' real behavior.

fMRI data acquisition and preprocessing

Whole-brain imaging was acquired using a Siemens 3T Magnetom Prisma system with a 64-channel head coil. First, a high resolution T1 weighted MPRAGE image was acquired for visualization (repetition time (TR), 1900 ms; echo time (TE), 3.02 ms; flip angle, 9°; 160 sagittal slices; 1 x 1 x 1 mm voxels). Functional volumes were acquired using a gradient-echo echo planar sequence (TR, 2000 ms; TE, 28 ms; flip angle 90°; 38 interleaved axial slices tilted approximately 15° from the AC-PC plane; 3 x 3 x 3 mm voxels). Functional data were acquired over three runs. Each run lasted 16.5 min on average (Mean: 494.8 acquisitions). After the functional runs, a brief in-plane anatomical T1 image was collected, which was used to define a brain mask that respected the contours of the brain and the space of the functional runs (TR, 350 ms; TE 2.5 ms; flip angle 70°; 38 axial slices; 1.5 x 1.5 x 3 mm voxels). Soft padding was used to restrict head motion throughout the experiment. Stimuli were presented on a 32-inch monitor at the back of the bore of the magnet, and subjects viewed the screen through a mirror attached to the head coil.

Functional data were preprocessed using SPM12. Quality assurance for the functional data of each subject was first assessed through visual inspection and TSdiffAna (https://sourceforge.net/projects/spmtools/) and ArtRepair

453 (http://cibsr.stanford.edu/tools/human-brain-project/artrepair-software.html). Outlier
454 volumes (defined by standard deviations from the global average signal) were interpolated
455 after preprocessing. Slice timing correction was carried out by resampling all slices to match
456 the first slice. Next, motion during functional runs was corrected by registering volumes to
457 the mean using rigid-body transformation. In any case where movement across runs was in
458 excess of the voxel size in any direction (3 mm), realignment was recalculated run-by-run.
459 Any participants where motion within a run was larger than a voxel were excluded from
460 further analysis (N = 2). Functional volumes were then normalized to Montreal Neurological
461 Institute (MNI) stereotaxic space using 4th order B-spline interpolation, and resampled to 2
462 x 2 x 2 mm voxels using trilinear interpolation. Finally, volumes were spatially smoothed
463 using an 8 mm full-width half-maximum isotropic Gaussian kernel. The in-plane anatomical
464 T1 image for each subject was normalized to MNI space and used to create a brain mask for
465 functional analysis using the Brain Extraction Tool in FSL
466 (https://fsl.fmrib.ox.ac.uk/fsl/fslwiki/).

467 *fMRI data analysis*

468 Functional data were analyzed under the assumptions of the GLM using SPM12. All
469 regressors and parametric modulators were convolved with the SPM canonical
470 hemodynamic response function (HRF). Subject motion (six translational and rotational
471 components) were also included as nuisance regressors. Beta coefficients for single subject
472 effects were estimated using a fixed-effects model in a first-level analysis. For whole-brain
473 contrasts, these estimates were then included in a second-level analysis using a one-sample
474 t-test against 0 at each voxel. Whole brain t-statistic maps were thresholded at a cluster
475 defining threshold of $P < 0.001$ uncorrected, and then evaluated for statistical significance at

476 the cluster corrected FWE threshold of $P < 0.05$ to control for multiple comparisons. The
477 cluster extent for this threshold varied by test and is reported with each analysis.

478 *fMRI general linear models*

479 Three different general linear models (GLMs) were fit to fMRI data:

480 (1) Condition-based GLM

481 The condition-based GLM included separate regressors at the response and feedback
482 phases for the following factors: clustering (recipe, independent), value (positive, negative),
483 presentation number (1, 2, 3) and accuracy (correct, error). The duration of the boxcar for
484 the response regressors was set to the median of subjects' combined reaction time and slider
485 movement durations. Trial-by-trial deviation from this median duration was included as an
486 additional nuisance regressor. This GLM also included a nuisance regressor for the time the
487 stimulus display was on screen (i.e. the response window, ISI and feedback).

488 (2) Finite impulse response GLM

489 For ROI-based analyses on contrasts of task conditions, a separate finite impulse
490 response (FIR) GLM was fit to each participant. This model had the identical conditions as
491 the condition-based GLM described immediately above, but used an FIR model with eight
492 time points (16 s window) as a basis function for the hemodynamic response function. This
493 allowed us to measure activity within these ROIs without making assumptions about the
494 shape of the hemodynamic response function.

495 (3) Model-based value components GLM

496 Finally, we tested for correlates of model-based value terms and their interaction
497 with participants' value ratings (i.e. participant-P(yes)) using a parametric GLM. This model
498 had three boxcar regressors: a response regressor with onsets at stimulus presentation and

499 durations lasting to the point participants finished moving the slider, a feedback regressor
500 with onsets and durations lasting the presentation of feedback, and a nuisance regressor for
501 the stimulus display. There were eight parametric modulators on the response regressor:
502 participant-P(yes), participant confidence, experienced value, schema value, unfamiliarity,
503 interactions between participant-P(yes) and experienced value, schema value and
504 unfamiliarity, as well as subjective value ratings for ingredients. These interactions served
505 as a filter to focus on neural activity that responded to the influence of these model-based
506 terms on participants' value judgments. The feedback regressor also had two parametric
507 modulators: reward prediction errors (RPE; calculated as the difference between
508 participant-P(yes) and outcomes) and surprise (calculated as the absolute value of RPEs).
509 Parametric modulators were not orthogonalized in this model.

510 *Region of interest analyses*

511 Regions of interest (ROIs) were defined for testing region-specific hypotheses using
512 unbiased criteria. These ROIs were either defined using masks from the automated
513 anatomical labelling atlas (AAL), or using 10 mm spheres around peak coordinates from
514 independent studies. These spheres were then masked to only include voxels that were more
515 than 50% likely to be gray matter in SPM's tissue probability map. The coordinates and
516 references for these ROIs are listed in Table 1.

517 In ROI analyses contrasting conditions, the time course of activity within each ROI
518 was estimated using the MarsBar Toolbox (Brett, Anton, Valabregue, & Poline, 2002) from
519 the FIR GLM. For each ROI, the peak activity was found across conditions and subjects, and
520 the mean activity ± 1 bin around this time point was extracted and tested using RM-ANOVAs.

521 In ROI analyses of parametric GLM models, the mean beta weights within ROI voxels were
522 extracted instead.

523 **Table 1.** Description of ROIs

Region of interest	Definition	Center of mass (MNI)
vmPFC	Positive>Negative effects of subjective value (Bartra, McGuire, & Kable, 2013), masked using AAL definition of vmPFC from same reference	-1, 44, -7
mPFC	10 mm sphere around peak activation in a preference construction task (Barron, Dolan, & Behrens, 2013)	-6, 53, 13
HPC	Left and right hippocampal AAL masks (Tzourio-Mazoyer et al., 2002)	
Striatum	Left and right putamen and caudate AAL masks	
aVLPFC	10 mm sphere around peak activation in semantic retrieval task (Badre, Poldrack, Pare-Blagoev, Insler, & Wagner, 2005a)	-54, 27, -9
MTC	10 mm sphere around peak activation in semantic classification task (Thompson-Schill, D'Esposito, Aguirre, & Farah, 1997)	-52, -55, 2

524
525 *Generalized psychophysical interaction analysis*

526 Generalized psychophysical interaction (gPPI) analyses were carried out using the
527 CONN toolbox in conjunction with SPM12 (Whitfield-Gabrieli & Nieto-Castanon, 2012). The
528 same ROIs described in Table 1 were used as seeds for focused ROI-ROI connectivity
529 analyses and exploratory whole-brain analyses. Task-related activity was regressed out
530 using the condition-based GLM described above, including six regressors for translational
531 and rotational motion and trial-by-trial deviations from the median of reaction time and
532 slider movement durations, as well as additional nuisance regressors including five principal
533 components for both cerebrospinal fluid voxels and white matter, and a regressor for linear

trends in the signal. The residuals of this model were then high-pass filtered at 0.008 Hz and used in the analysis of functional connectivity.

gPPI analyses involved a two-step process. In a first-level analysis, connectivity between *a priori* pairs of ROIs was measured as the bivariate correlation between the mean residuals of voxel activities. In a second level analysis, correlation coefficients for each ROI-ROI in each subject were Fisher transformed and subjected to a one-sample *t*-test against zero. Exploratory seed-to-voxel whole brain connectivity analyses were similarly carried out by calculating the bivariate correlation of mean residual activity within an ROI and all other voxels in each subject. These correlations were then Fisher-transformed and compared to zero with one-sample t-tests. As with above fMRI analyses, all whole-brain effects were first peak thresholded at $P < 0.001$ and further thresholded at FWE cluster corrected threshold of $P < 0.05$ to control for multiple comparisons. Cluster thresholds are reported separately for each analysis.

Results

Behavioral data

To test if participants took advantage of schematic knowledge to make decisions, we first examined whether participants choices reflected customers' recipe preferences on the first presentation of ingredients before seeing any external feedback (Figure 3a). On these trials, participants accepted ingredients associated with the positive value recipe more often than ingredients associated with the negative value recipe and more often than positive value independent ingredients. This was evident in a significant three-way interaction between value, clustering and presentation number on participants' choices (RM-ANOVA: F

$_{2,\ 44}$ = 27.20, P < 0.0001, $\eta_p^2 = 0.55$), and direct contrasts between the ingredient types (Bonferroni corrected t-tests: $t(22) \geq 7.79$, P's < 0.0001, d's ≥ 1.62).

In contrast, there was no significant difference between acceptance rates for positive and negatively valued independent ingredients on the first presentation. This was as expected, as the ingredients in this condition did not have inferable value based on an association with a positive or negative recipe. The interaction between value and clustering on participants' choices was confirmed with a separate RM-ANOVA on the first presentation only ($F_{1,22} = 61.31$, $P < 0.0001$, $\eta_p^2 = 0.73$). Participants accepted ingredients associated with the negative value recipe numerically less often than negative independent ingredients, but this difference was not significant after correction for multiple comparisons. Overall, the choice results indicate that participants successfully inferred value information from recipe associations, though these effects were stronger for the positively valued recipe.

There was clear evidence that participants learned ingredient values from feedback. Participants made choices consistent with the values of ingredients more often in the second and third presentations than in the first in all conditions, demonstrating retention of feedback from previous trials (Bonferroni corrected t-tests: t's$(22) \geq 4.54$, P's < 0.01, d's ≥ 0.95). Similarly, participants' rate of value consistent choices increased significantly from the second presentation to the third in all conditions, except for independent positive ingredients (Bonferroni corrected t-tests: t's$(22) \geq 4.69$, P's < 0.01, d's ≥ 0.98).

Notably, participants also tended to reject both positive and negative independent ingredients in the first presentation significantly more often than chance (One sample t-tests: t's$(22) \geq 8.69$, P's < 0.0001, d's ≥ 1.81). Thus, participants strategically avoided endorsing independent ingredients before learning their values through feedback.

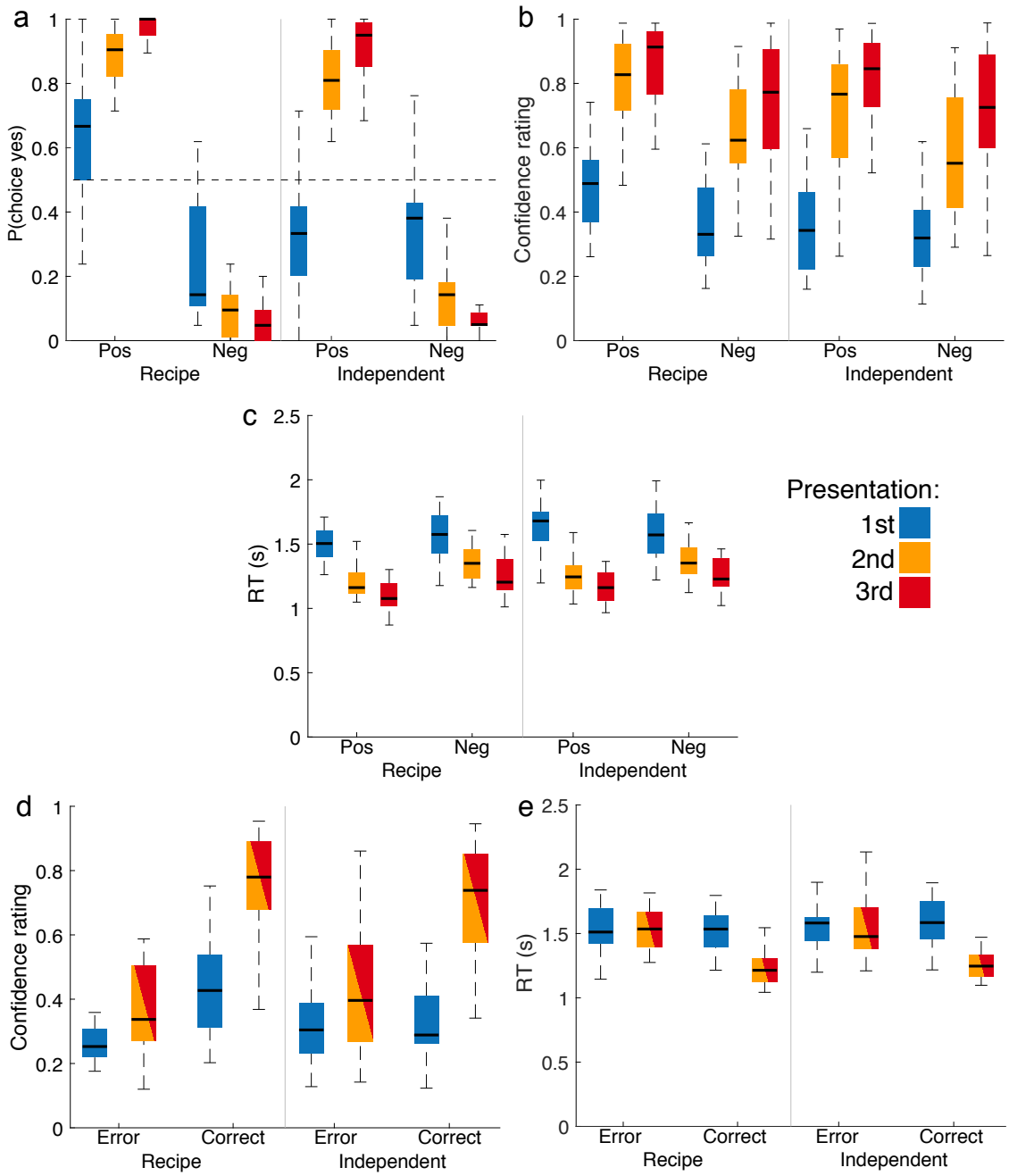

Figure 3. Behavioral data**.** Choices, reaction times (RT) and confidence ratings for positive (pos) and negative (neg) ingredients in the recipe and independent conditions across presentations. **a.** Frequency of 'yes' choices, **b.** Confidence ratings for correct responses. **c**. Reaction times for correct responses in recipe and independent conditions, for positive (pos) and negative (neg) ingredients. **d.** Confidence ratings for errors and correct responses in recipe and independent conditions, collapsing across value. Second and third presentations are also collapsed. **e.** Reaction times for correct and error responses in the same conditions as **d**. Boxes represent 25th, 50th and 75th quantiles of the data. Whiskers are approximately ±2.7 SD.

579

To test how participants' belief in their choices changed during the task, we next examined how reported confidence changed on correct responses (Figure 3b). Confidence increased with repeated presentations, and was also greater overall for recipe and positive value ingredients (RM-ANOVA: F's ≥ 27.88, $P \leq 0.0001$, $\eta_p^2 \geq 0.58$). Confidence for acceptance of positive recipe ingredients was significantly higher than positive independent ingredients on the first presentation (Bonferroni corrected t-test: $t(20) = 4.57$, $P < 0.01$, $d = 0.99$) and third presentation (Bonferroni corrected t-test: $t(20) = 4.96$, $P < 0.01$, $d = 1.08$). However, there was no comparable difference in confidence for rejections of negative recipe and independent ingredients, resulting in a significant interaction between clustering and value (RM-ANOVA: $F_{1, 20} = 9.28$, $P = 0.006$, $\eta_p^2 = 0.32$),

Confidence also increased significantly from the first presentation to the second and third presentations in all conditions (Bonferroni corrected t-tests: t's(20) ≥ 4.57, P's ≤ 0.01, d's ≥ 1.29), and from the second to the third presentation in all conditions, except for negative recipe ingredients (Bonferroni corrected t-tests: t's(20) ≥ 3.98, P's ≤ 0.05, d's ≥ 0.87), leading to a modest interaction of value and presentation number ($F_{2, 40} = 3.34$, $P = 0.04$, $\eta_p^2 = 0.14$).

Similar to reported confidence, participants' reaction times were also strongly influenced by experience with ingredients with stronger decrements in subsequent presentations of positive recipe ingredients (Figure 3c). There was a significant interactions between value with presentation number ($F_{2, 40} = 8.50$, $P = 0.0008$, $\eta_p^2 = 0.30$), with larger drops in reaction times for positive ingredients, consistent with better recall. There was also an interaction between value and clustering (RM-ANOVA: $F_{1, 20} = 4.66$, $P = 0.04$, $\eta_p^2 = 0.19$), owing to comparatively bigger effect of value on recipe ingredients compared to

independent ingredients. Responses in the first presentation did not significantly differ by cluster condition or value.

In anticipation of analyzing the effects of memory retrieval failures on brain activity, we also tested if were associated with lower confidence and longer reaction times, as would be expected for retrieval failures. We collapsed across value levels and the second and third presentations to have enough error trials per participant for this analysis. Confidence ratings were influenced by significant interactions between accuracy and clustering (Figure 3d; RM-ANOVA: $F_{1, 21} = 15.43$, $P = 0.0007$, $\eta_p^2 = 0.42$), and accuracy and presentation number ($F_{1, 21} = 43.69$, $P < 0.0001$, $\eta_p^2 = 0.67$). On the first presentation, participants were significantly more confident on correct responses for recipe ingredients than independent ingredients (Bonferroni corrected t-tests: $t(21) = 3.77$, $P < 0.05$, $d = 0.80$), and error responses on recipe ingredients (Bonferroni corrected t-tests: $t(21) = 5.60$, $P < 0.01$, $d = 1.19$). There was no comparable significant difference in confidence for correct and error responses for independent ingredients in the first presentation. We confirmed that the effects of accuracy differed between clustering conditions on this first presentation by separately testing this interaction (RM-ANOVA: $F_{1, 21} = 14.34$, $P = 0.001$, $\eta_p^2 = 0.40$). Thus, confidence on the first presentation appeared to selectively depend on retrieval of relevant recipe associations. Confidence was also higher on accurate responses compared to errors on the second and third presentations of both recipe and independent ingredients (Bonferroni corrected t-tests: t's$(21) \geq 6.64$, P's < 0.0001, $d = 1.42$).

Reaction times were influenced by an interaction of accuracy and presentation number (Figure 3e; RM-ANOVA: $F_{1, 21} = 49.84$, $P < 0.0001$, $\eta_p^2 = 0.70$), but there was only a trend toward an interaction between accuracy and clustering ($F_{1, 21} = 3.81$, $P = 0.06$, $\eta_p^2 =$

625 0.15), and no three-way interaction. Participants were significantly faster on correct
626 responses than errors on the second and third presentations of both recipe and independent
627 ingredients (Bonferroni corrected t-tests: t's(21) ≥ 5.03, P's < 0.01, d ≥ 1.07). This pattern is
628 consistent with longer reaction times on errors reflecting retrieval failures (Ratcliff, 1978).
629 In contrast, there were no significant differences in reaction times for correct and error
630 responses in the first presentation for either clustering condition.

631 In summary, behavioral results established that participants were able to infer the
632 value of ingredients based on their recipe association and used these inferred values to make
633 choices. Participants also showed a generally risk averse attitude on this first presentation
634 by tending to reject independent ingredients. On subsequent presentations of an ingredient,
635 participants accurately retrieved explicit memory of deterministic feedback to make faster,
636 more confident decisions. This was the case across both recipe and independent items.
637 However, participants continued to benefit from recipe associations in these later
638 presentations, with generally faster reaction times and greater confidence for correct
639 responses in this condition compared to independent ingredients. Finally, participants
640 tended to asymmetrically utilize knowledge about the positive recipe more than the negative
641 recipe throughout all trials.

642 *Main effects of task conditions in whole-brain analyses*

643 We hypothesized that vmPFC and striatum would respond to schema-based and
644 experienced values of ingredients respectively, and interact with different memory systems
645 in retrieving and constructing these values. Thus, we predicted that vmPFC activity would
646 be modulated by schema values more than directly experienced values, and the opposite
647 would be true of the striatum. We also predicted that a network of regions, including the

striatum, HPC and middle temporal cortex would be engaged by successful retrieval (Spaniol et al., 2009), while aVLPFC would be engaged by retrieval difficulty (Badre, Poldrack, Pare-Blagoev, Insler, & Wagner, 2005b). We first tested how ingredient clustering, value, presentation number and accuracy affected activity using simple contrasts from our condition-based GLM at a whole-brain level (Table 2). These analyses were filtered to focus on correct responses, excluding trials where participants may have made errors due to failure to appropriately recall information relevant to ingredient values, except where trials with different response accuracy were directly contrasted.

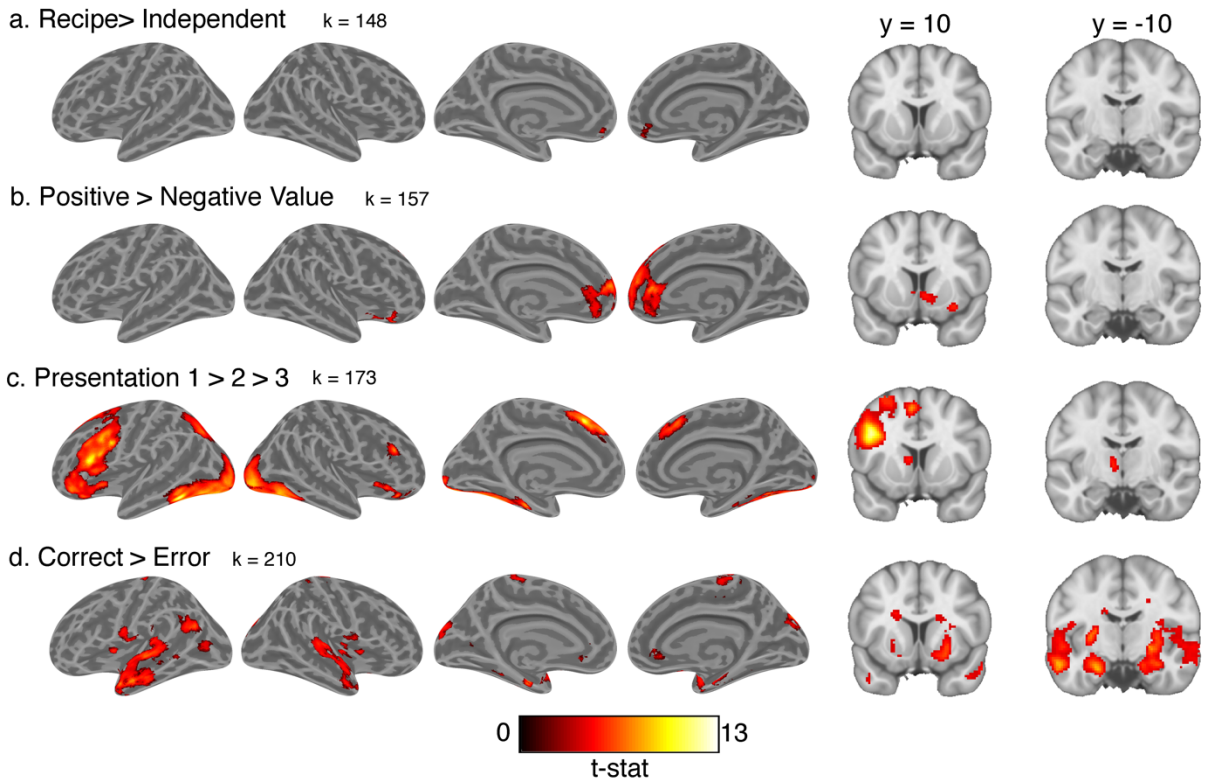

Figure 4. Whole brain contrasts projected onto inflated cortical surfaces and coronal slices for main effects of **a**. ingredient-recipe clustering, **b**. ingredient value, **c**. presentation number and **d**. response accuracy. All images are thresholded at $P < 0.05$, FWE cluster corrected. All main effects, except for accuracy, are filtered to only include correct responses. Cluster extent threshold for each contrast is given by value of k.

657 Recipe ingredients elicited greater activity than independent ingredients in medial
658 OFC (Figure 4a), but not elsewhere. Ingredients associated with positive value elicited
659 greater activity in OFC and medial PFC, as well as the ventral striatum (Figure 4b). Compared
660 with later ingredient presentations, the first encounter with an ingredient was associated
661 with widespread activity in lateral PFC, including left VLPFC, inclusive of the aVLPFC, and
662 the caudate nucleus (Figure 4c). Activity in left MTC, bilateral HPC and putamen was higher
663 in correct responses compared to errors across all presentations (Figure 4d).

664 **Table 2. fMRI activations for main effects of task conditions shown in Figure 4**

Region (AAL2)	MNI Coordinates			Number of voxels	Peak *t*-value
	x	y	z		
Recipe > Independent, correct (k = 148)					
Left superior frontal gyrus, medial orbital	-10	44	-12	240	4.31
Positive > Negative Value, correct (k = 157)					
Right anterior cingulate	12	40	8	4134	7.60
Left superior frontal gyrus, medial	-10	54	14		7.54
Right superior frontal gyrus, medial orbital	4	34	-14		5.84
Right posterior orbital gyrus	24	26	-14	282	5.78
Right caudate nucleus	6	12	-4	172	4.66
Presentation 1 > 2 > 3 (k = 173)					
Left inferior frontal gyrus, opercularis	-42	4	28	8816	12.39
Left supplementary motor area	-6	22	46		11.67
Left inferior frontal gyrus, triangularis	-46	24	16		11.30
Left inferior temporal gyrus	-48	-52	-16	4672	11.83
Left fusiform gyrus	-22	-86	-12		8.76
Left fusiform gyrus	-36	-70	-12		8.59
Right fusiform gyrus	36	-58	-12	3287	10.21
Right inferior occipital gyrus	34	-88	-6		8.51
Right fusiform gyrus	36	-28	-28		6.24
Right middle frontal gyrus	50	32	22	578	8.27
Left middle occipital gyrus	-24	-68	36		7.59
Left superior parietal gyrus	-30	-62	66		4.14
Right inferior frontal gyrus, orbital	32	30	-10	621	6.91

Left thalamus	-8	-8	4	370	5.36
Correct > error (k = 210)					
Right pallidum	26	-6	-6	4394	8.87
Right superior temporal gyrus	56	-26	4	4394	6.39
Right middle temporal gyrus	62	-2	-18	4394	6.13
Right paracentral lobule	10	-26	68	1065	5.29
Left precentral lobule	-22	-22	60	1065	4.61
Left middle temporal gyrus	-46	2	-28	6667	8.37
Left hippocampus	-24	-10	-22	6667	7.70
Left putamen	-30	-2	2	6667	7.68
Right superior occipital gyrus	24	-90	30	1195	7.21
Left cuneus	-8	-94	22	1195	5.31
Left anterior cingulate	-2	28	-8	241	4.54
Right superior frontal gyrus, medial	6	50	0	241	3.79

All reported clusters were significant at the $P < 0.05$, FWE-corrected threshold at the cluster level after peak thresholding at $P < 0.001$. The critical cluster extent threshold for each contrast is given by the value of k.

Region of interest analyses

To follow-up the whole-brain voxel-wise contrasts, we tested for more specific task-dependent changes in activity within a set of *a priori* regions of interest (ROIs) defined in Table 1 using a finite impulse response (FIR) model of the hemodynamic response. We were primarily interested in how the clustering status of ingredients influenced value-related activity across ingredient repetitions on correct responses. Here we focused on vmPFC and the striatum, since we had *a priori* expectations that these regions would differentially process value related to episodic and schematic memory. As the medial frontal wall is functionally heterogeneous (Braga & Buckner, 2017; Roy, Shohamy, & Wager, 2012), we included two ROIs from this region, one that was defined by a meta-analysis of studies of expected-value (Bartra et al., 2013), and a more dorsal ROI (mPFC) that responded to shared associations between components of a recipe schema in another experiment (Barron et al.,

2013). This dorsal mPFC ROI responded to ingredient value, but not any other task manipulations.

vmPFC was more active for positive than negative expected value, evident in a main effect of value (Figure 5a; RM-ANOVA: $F_{1,20} = 9.13$, $P = 0.007$, $\eta_p^2 = 0.31$), consistent with the whole-brain analysis. Activity in this region was greater for positive compared to negative recipe ingredients in the third presentation (Bonferroni corrected t-test: $t(20) = 4.90$, $P < 0.01$, $d = 1.07$), but there was no comparable value difference for independent ingredients (Bonferroni corrected t-test: $t(20) = 1.13$, $P > 0.05$, $d = 0.25$). There was no significant difference between vmPFC activity in response to positive and negative recipe ingredients on the first presentation, leading to a three-way interaction between value, presentation number and clustering ($F_{1,20} = 5.06$, $P = 0.01$, $\eta_p^2 = 0.20$). This null result of value on the first presentation was not merely due to the ROI selection; an exploratory whole-brain contrast of positive and negative recipe conditions on the first presentation in the condition-based GLM was similarly null. vmPFC activity was also generally higher in later presentations, reflected in a marginal main effect of presentation number ($F_{2,20} = 3.29$, $P = 0.05$, $\eta_p^2 = 0.14$), but there was no significant main effect of clustering ($F_{1,20} = 1.42$, $P = 0.2$, $\eta_p^2 = 0.06$).

Within the striatum ROI, there was greater activation for positive than negative value, evident in a strong main effect of value (Figure 5b; $F_{1,20} = 9.17$, $P = 0.007$, $\eta_p^2 = 0.31$), consistent with the observation from the whole brain voxel-wise analysis. However, there were no other significant main effects or interactions.

We hypothesized that value judgments in this task would rely on different neural systems supporting different types of memory. In particular, we predicted that retrieval of values associated with independent ingredients learned through feedback would place

704 greater demands on the HPC, while the MTC would be involved more in trials where
705 semantic memory about recipes was needed to infer ingredient values and aVLPFC would be
706 engaged by greater retrieval demands on the first presentation. To test these predictions, we
707 evaluated the effects of clustering status, presentation number and accuracy in ROI-based
708 analyses of the HPC, MTC and aVLPFC. We collapsed across value conditions and combined
709 presentations two and three into a single level to have enough error trials for this analysis.

710 HPC activity was greater on accurate trials, confirming the whole-brain results
711 (Figure 5c; RM-ANOVA: $F_{1,21} = 13.14$, $P = 0.002$, $\eta_p^2 = 0.38$). HPC activity was also generally
712 lower on later presentations ($F_{1,21} = 6.54$, $P = 0.02$, $\eta_p^2 = 0.24$). The effect of accuracy on HPC
713 activity was modulated marginally by clustering ($F_{1,21} = 4.65$, $P = 0.04$, $\eta_p^2 = 0.18$).
714 Surprisingly, we found greater HPC activity on correct trials than error trials for recipe
715 ingredients, collapsing across presentations (Bonferroni corrected t-test: $t(21) = 3.47$, $P <$
716 0.01, $d = 0.74$), but no such accuracy effect for independent ingredients. There was no main
717 effect of clustering, or three-way interaction of clustering, accuracy and presentation.

718 MTC activity responded to an interaction of clustering and presentation number
719 (Figure 5d; $F_{1,21} = 5.60$, $P = 0.03$, $\eta_p^2 = 0.21$). Posthoc tests collapsed across accuracy revealed
720 a significantly greater reduction in MTC activity for independent ingredients in the second
721 and third presentations compared to the first presentation (Bonferroni corrected t-test:
722 $t(21) = 2.87$, $P < 0.05$, $d = 0.61$), but no significant difference for recipe ingredients. While
723 MTC seemed to be engaged on the first presentation in all conditions, this reduced in
724 subsequent presentations for independent ingredients, consistent with less reliance on
725 semantic knowledge in this condition.

726

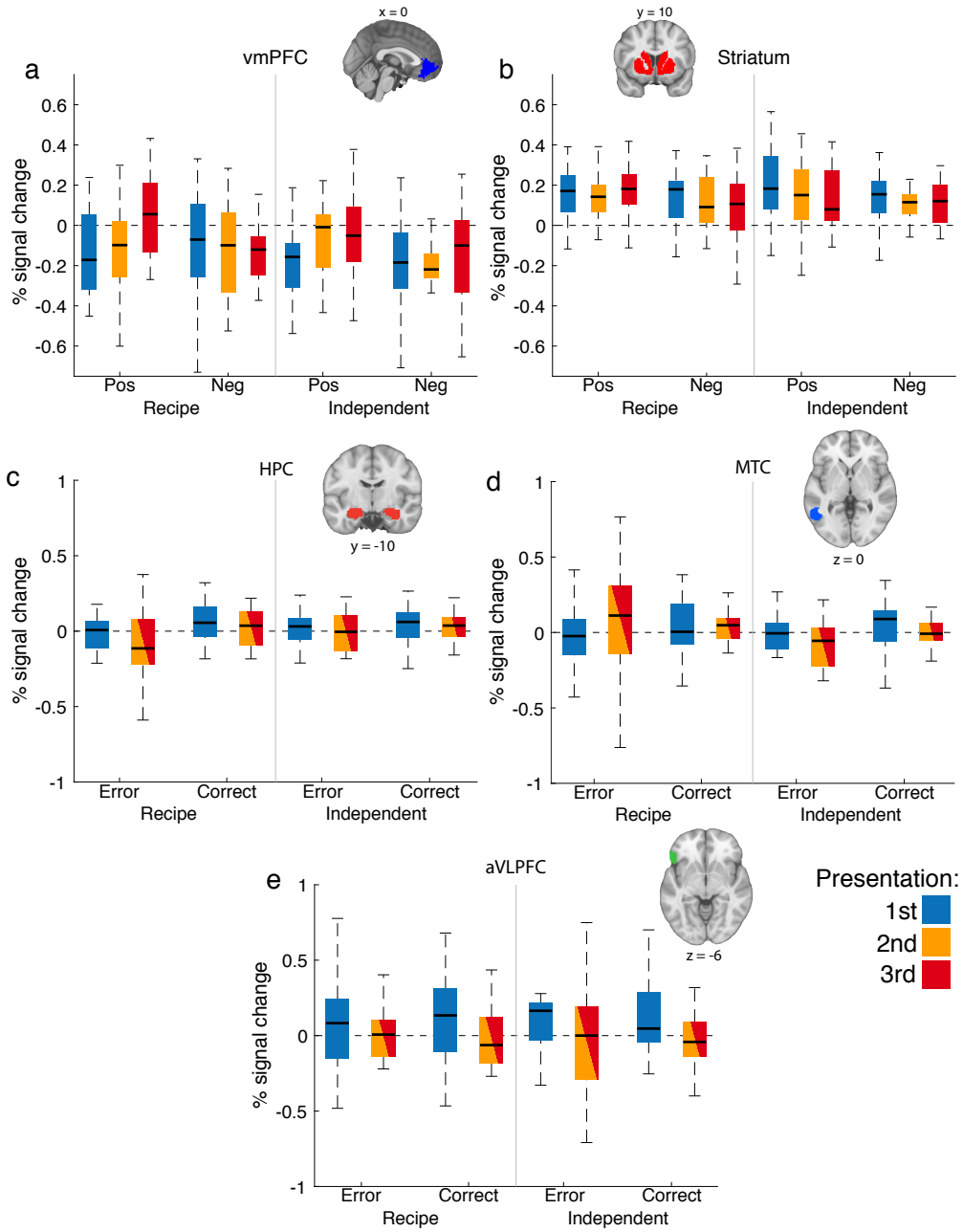

Figure 5. Region-of-interest analyses showing percent signal change in **a.** ventromedial prefrontal cortex (vmPFC) and **b.** the bilateral striatum across conditions for correct responses. **c.** Percent signal change in the hippocampus (HPC) for correct and erroneous responses, collapsed across value conditions. Second and third presentations are collapsed. **d.** Middle temporal cortex (MTC) and **e.** anterior ventrolateral prefrontal cortex (aVLPFC), same conditions as **c**.

727 aVLPFC activity was larger on the first presentation compared to the second and
728 third, consistent with the whole-brain analysis, revealed in a main effect of presentation
729 number (Figure 5e; $F_{1, 21} = 10.76$, $P = 0.004$, $\eta_p^2 = 0.34$). The response of aVLPFC did not
730 change with accuracy or clustering status, or with any interaction between task variables.

731 In summary, ROI-based analyses confirmed whole-brain contrasts demonstrating
732 that the vmPFC and striatum carried information about ingredient values. Unlike the
733 striatum, value-related activity in vmPFC was greater for recipe ingredients compared to
734 independent ingredients in later presentations, but not in the first presentation where the
735 demand for inferring ingredient values from recipe associations was the greatest. In line with
736 our predictions, the MTC responded to differential demands on semantic memory, though
737 this was only true in later presentations. aVLPFC activity reduced in subsequent
738 presentations overall, in line with engagement by increased retrieval demands. While the
739 HPC responded differentially to retrieval success and failures in later presentations, this
740 effect was surprisingly greater for recipe ingredients than independent ingredients, possibly
741 due to the stronger encoding of these recipe ingredients, evident in participants' behavior
742 on these trials.

743 *Computational model comparison*

744 We had hypothesized that vmPFC would be preferentially engaged by schema-based
745 values, while the striatum would be involved in evaluating the contents of episodically
746 encoded value information. While value-related differences in vmPFC activity grew larger in
747 later presentations of recipe ingredients compared to independent ingredients, this change
748 in activity could not be easily differentiated from value information learned from feedback.
749 Importantly, this condition-based analysis also ignores the continuous nature of associations

between independent ingredients and recipes. For example, strawberries are considered part of the 'cake' cluster, but also have some association with 'pie.' Further, filtering trials by accuracy based on participant responses and task-defined values ignores that responses to independent ingredients on the first presentation are made without any useful experienced or schematic value information, and ignores systematic biases or strategies participants may use in making choices that are not explicitly captured by our experimental design (e.g. a bias against endorsing independent ingredients on their first presentation).

To better separate these components of expected value for testing our first two hypotheses regarding the neural systems supporting valuation of information from different memory sources, we developed a computational model of behavior to estimate the contribution of information learned directly from experience and inferred from schematic associations to participants' choices in each trial. We then used these values in a model-based parametric GLM to determine the correlates of this information during value judgment.

Our computational model of behavior made a few basic assumptions about learning in this task that are described in more detail in the Materials and Methods section. Briefly, each ingredient had an 'experienced value' (*EV*), which depended on feedback and decayed over time, and a 'schema value' (*SV*), which was derived from the differences in associative strength between an ingredient and the positive and negative recipes. The associative strength of an ingredient with each recipe was based on a latent semantic analysis of normative ingredient-recipe associations (Dumais, 2004; Landauer et al., 1998). Each of these value terms were weighted by a temperature parameter that determined their contribution to the model's output, a continuous estimate of the probability that it would endorse an ingredient, which we will refer to as model-P(yes).

Starting with these assumptions, we followed a step-wise process of adding parameters to a model with these features and comparing the AIC of the new model against the best simpler model. This allowed us to test if the new model better explained participants' behavior while penalizing for the addition of a new parameter. Figure 6 shows the AIC scores for these alternative models against the base model. Please see the methods section for a fuller accounting of the parameters in the best fitting model and alternative models in this figure.

The final best fitting model allowed for a more sophisticated parameterization of SV where the number of dimensions in the latent semantic analysis of recipe-ingredient associations was allowed to vary. This parameter essentially controlled the depth of recipe information considered in computing *SV* (from simple distinctions like savory-sweet to more fine-grained information about particular recipes; Figure 2). The model also allowed participants' perception of the similarity of an ingredient's associations with positive and negative recipes to act as a weight on the respective contributions of the difference and sum of these associations in the calculation of *SV*. This enabled the model to determine whether ingredients, like the strawberry example above, would be attributed positive, negative, or null value if it had a strong association with both the positive and negative recipes (e.g. cake and pie).

Unfamiliarity with an ingredient was also allowed to influence decisions about betting or passing in the best fitting model. Unfamiliarity was operationalized as the opposite of the unsigned experienced value of items. In other words, unfamiliarity was highest when ingredients were seen on the first presentation, or when ingredients had not been seen for many trials and memory for their experienced value had decayed. This parameter thus

effectively accounted for variance in participants' willingness to bet on ingredients when information about their experienced values was weaker. Lastly, an additional free parameter acted as an intercept term in the decision function, which effectively acted as a fixed bias on the model's tendency to bet on ingredients.

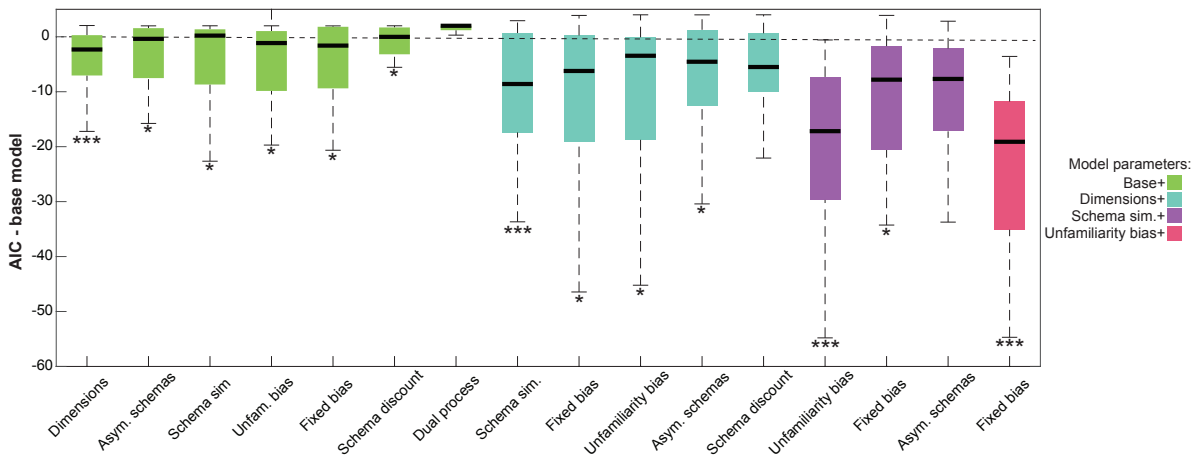

Figure 6. Difference in model Akaike Information Criteria (AIC) compared against base model. Model parameters were added in a step-wise process where the parameters that best improved on the previous best fitting model were added to the next step (indicated in the legend). See Materials and Methods section for a more complete description of these models. *, $P < 0.05$, one-tail t-test indicating significant improvement on previous best fitting model. ***, best model within a step and significant improvement.

Computational model validation

To ensure that our computational model was capturing participants' decisions and understand how it was accomplishing this, we carried out a series of analyses to validate its parameters and behavior. We first examined if there were general tendencies for the two bias and schema similarity temperature parameters towards positive or negative values by conducting two-tailed, one-sample t-tests against zero (Table 3). While the unfamiliarity bias parameter was significantly lower than zero ($t(22) = 3.91$, $P = 0.0008$, $d = 0.81$), the opposite was true of the fixed bias parameter ($t(22) = 3.18$, $P = 0.004$, $d = 0.66$). The schema similarity temperature parameter was not significantly different from zero ($t(22) = 0.90$, $P = 0.4$, $d =$

0.19). Thus, the unfamiliarity temperature parameter captured participants' aversion to betting on ingredients on their first presentation or when memory for these ingredients was weak, while the fixed bias parameter exerted a uniform inverse tendency across all trials, moving the model towards endorsing ingredients in opposition to the unfamiliarity parameter.

Table 3. Mean parameter values and Pearson correlations between parameters in the best-fitting behavioral model

	Mean (SD)	**Decay**	**EV temp.**	**SV temp.**	**Schema similarity temp.**	**UF temp.**	**Fixed bias**
Decay	**0.02 (0.01)**	-					
EV temp.	**5.05 (0.32)**	0.35	-				
SV temp.	**2.07 (1.42)**	0.05	0.02	-			
Schema similarity temp.	**0.33 (1.75)**	-0.27	-0.01	0.25	-		
UF temp.	**-0.81 (0.99)**	0.09	0.31	0.31	0.06	-	
Fixed bias	**0.55 (0.83)**	0.15	-0.17	-0.45*	-0.47*	-0.85***	-
Recipe dimensions (log-space)	**2.56 (1.04)**	-0.04	0.07	0.60**	0.21	-0.04	-0.11

Experienced value (EV), schema value (SV), unfamiliarity (UF), *$P < 0.05$, **$P < 0.01$, ***$P < 0.001$

We also examined the covariance between parameters recovered from fitting this model to participants' behavioral data to test their independence (Table 3). The fixed bias parameter was negatively correlated with *SV* temperature, the schema similarity temperature, and the memory bias parameter. There was also a positive correlation between the recipe dimensions and *SV* temperature parameters, likely due to the cosine similarities between ingredients growing smaller on average with higher recipe dimensions (Figure 2).

To confirm that all of these parameters could be uniquely recovered in our model fitting procedure, we generated 100 simulated participants with randomly assigned parameters using the best fitting model. We reliably and accurately recovered all parameters in these data, with high correlations between simulated and recovered parameters (Pearson r's(98) ≥ 0.99, P's < 0.0001). However, as these data were simulated from randomly generated parameters, they did not share the covariance structure of the parameter estimates fit to participants' behavior described above. To assure that we could recover these parameters with the same covariance, we fit the model to simulated data generated using parameter estimates from the model fit to participants' behavior. For all seven parameters, there was a perfect correlation between the parameter estimates from participants' behavior and the simulated data (Pearson r's(21) = 1.00, P's < 0.0001).

Finally, we generated simulated behavior from the model using participants' recovered parameters to test that the model recapitulated key features of participants' behavior across task conditions. To directly compare the model and participants' behavior, we focused on participants' continuous estimate of whether or not they should endorse an ingredient, based on position of the slider between the 'yes' and 'no' ends of the bar (i.e. participant-P(yes)). We compared these ratings to the model-P(yes) measure, and transformed model-P(yes) to confidence based on the distance from the point of maximum uncertainty (i.e. 0.5). Participant-P(yes) ratings followed a similar pattern to their averaged binary choices, including key features on the first presentation like higher P(yes) for positive recipe ingredients compared to negative recipe, and positive independent, ingredients, and a bias against endorsing independent ingredients (data not shown)

We analyzed model-P(yes) and confidence ratings in the same way as participants' responses. Like with participants' choices, there was a strong three-way interaction between value, clustering and presentation number (Figure 7a; RM-ANOVA: $F_{2,44} = 53.82$, $P < 0.0001$, $\eta_p^2 = 0.71$). The model used recipe information to make decisions on the first presentation, with higher model-P(yes) ratings for positive recipe ingredients over negative recipe ingredients, and over independent positive ingredients (Bonferroni corrected t-tests: t's(22) ≥ 7.38, P's < 0.0001, d's ≥ 1.54). There was also no significant difference in model-P(yes) for positive and negative independent ingredients on this first presentation. Unlike real participants, the model gave significantly lower ratings to negative recipe ingredients than negative independent ingredients on the first presentation (Bonferroni corrected t-test: $t(22) = 6.64$, P < 0.0001, $d = 1.38$), suggesting that it used information about the negative recipe more than participants did. In subsequent presentations, the model also followed the values of options learned through feedback, hewing closer to ingredient values in presentation two and three compared to one (Bonferroni corrected t-tests: t's(22) ≥ 9.23, P's < 0.0001, d ≥ 1.93), and presentation three compared to two (Bonferroni corrected t-tests: t's(22) ≥ 5.72, P's < 0.01, d ≥ 1.19).

Similarly, we examined whether the model's predicted confidence followed the same pattern as participants' responses across task conditions on trials where participants responded correctly (Figure 7b). Model confidence rose predictably with presentation number (RM-ANOVA: $F_{2,40} = 150.65$, $P < 0.0001$, $\eta_p^2 = 0.88$), and was higher overall for recipe ingredients than independent ingredients ($F_{1,20} = 46.18$, $P < 0.0001$, $\eta_p^2 = 0.70$), however there was only a trend toward a main effect of value ($F_{1,20} = 3.45$, $P = 0.08$, $\eta_p^2 = 0.15$). Model confidence was also notably higher for both positive and negative recipe ingredients compared to independent ingredients on the first presentation (Bonferroni corrected t-tests: t's(20) ≥ 4.02, P's < 0.05, d's ≥ 0.88), rather than just positive recipe ingredients.

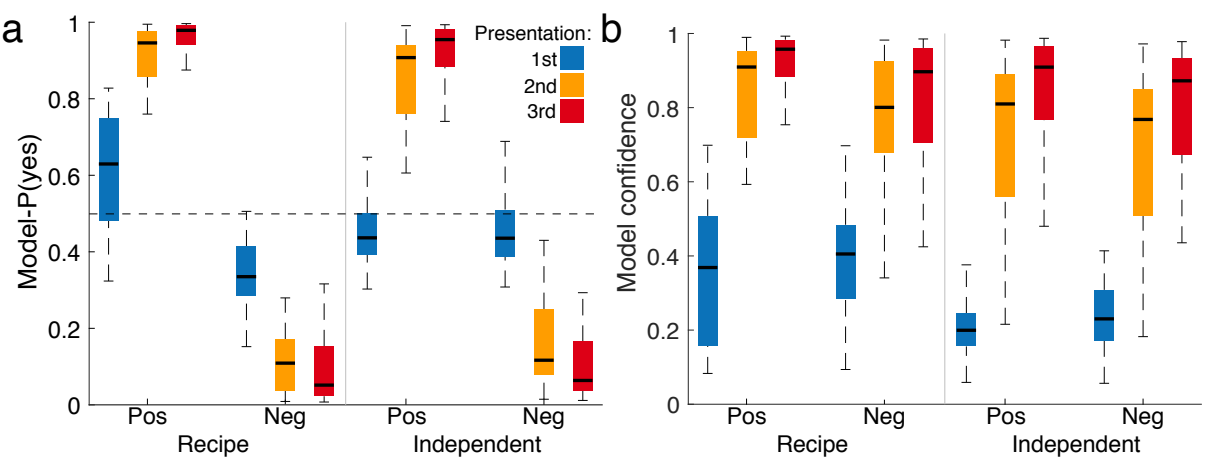

Figure 7. Model behavior across task conditions. **a.** Model-P(yes), a continuous indicator of the model's estimate of the value of these options. **B.** Model confidence on correct responses only.

In summary, our model captured core aspects of participants' behavior in this task, including utilization of recipe-based values and a bias against endorsing independent ingredients on the first presentation. The model was also able to recreate the basic pattern of participants' reported confidence rising with repeated presentations, with benefits for positive value and recipe associations. However, the model gave greater weight to the negative value recipe than participants and underestimated the effects of value on

878 confidence. While an alternative model with asymmetric weights for positive and negative
879 recipes improved model fitness, this addition did not survive our model selection process
880 (Figure 6), possibly due to variance between participants in the extent of this asymmetry.

881 *Model-based fMRI*

882 We had hypothesized that vmPFC would be engaged more by values inferred from
883 schematic associations than directly experienced values, which we hypothesized would be
884 tracked by activity in the striatum. Our computational model showed that ingredient values
885 could be captured by a combination of experienced value, schema value and unfamiliarity,
886 and allowed us to leverage these terms in testing these hypotheses by examining their
887 correlates in brain activity.

888 To focus on brain activity that responded to the influence of these model-based value
889 terms on participants' value judgments, we included interactions between these three terms
890 and participant-P(yes) in our GLM. These interactions selectively captured activity that
891 responded to the conjunction (or agreement) between the participants' responses with
892 experienced and schema values (e.g. when schema value was high and participant-P(yes)
893 were high, or when both were low). The interaction of unfamiliarity with value ratings
894 similarly let us capture where activity increased in response to higher participant-P(yes)
895 when unfamiliarity was high, or lower participant-P(yes) when unfamiliarity was low. In
896 doing so, we could focus on activity where behavior and model predictions were in
897 agreement. In contrast, the main effects of these model-based terms only captured the extent
898 to which correlates of this information were present in the brain, independent of
899 participants' response. This analysis may seem circular, as we are looking for correlates of
900 an interaction between these model-based terms with the behavior to which these terms

were fit. However, the fMRI correlates that are the dependent measure in this analysis were not part of the model fitting, breaking any potential circularity in our results. This GLM also included parametric modulators for participants' confidence ratings and participants' subjective value ratings (provided separately in a different task) on the response regressor as nuisance terms.

Whole-brain cluster corrected analyses found no significant main effects of participant-P(yes), experienced or schema-based value, or participants' subjective value ratings. There were significant correlates for the main effect of unfamiliarity, with increased activity in lateral PFC, visual cortex and several other regions, similar to the main effect of presentation number in the condition-based contrast above. There were also significant main effects for response confidence in the superior frontal gyrus and visual cortex (Table 4).

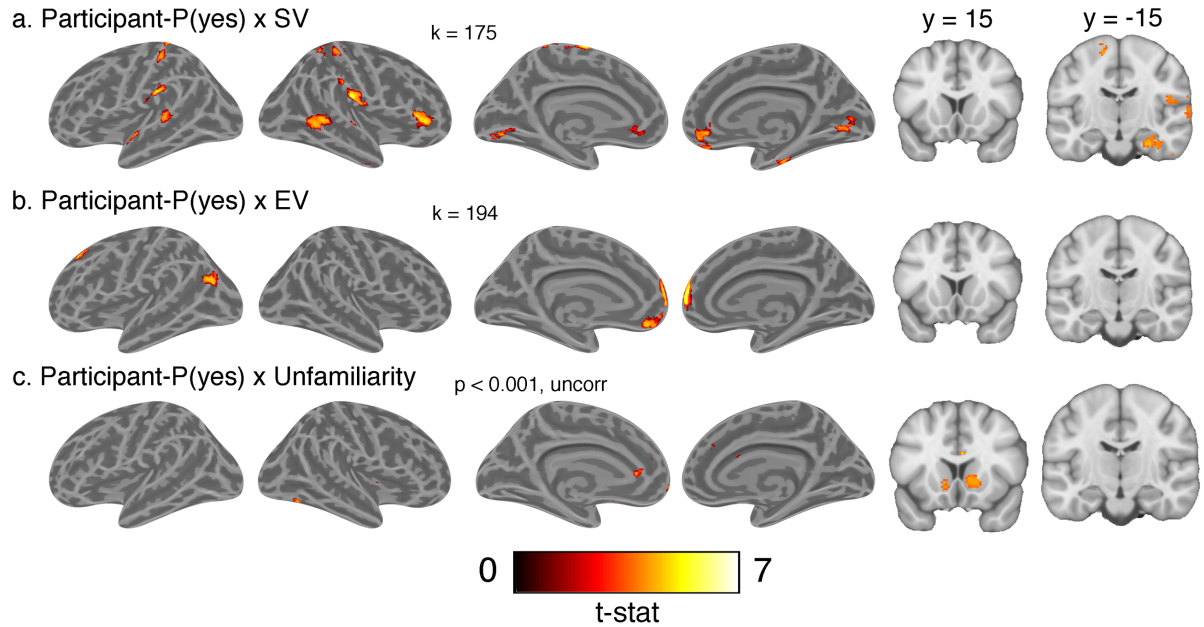

Figure 8. Whole brain t-statistic maps for interactions of model-based terms with participant-P(yes). **a.**. Interaction of participant-P(yes) and schema value (SV), **b.** Interaction of participant-P(yes) and experienced value (EV), **c**. Interaction of participant-P(yes) and unfamiliarity. All images are thresholded at $P < 0.05$, FWE cluster corrected, except for those shown in **c**. Cluster extent threshold for each map is given by value of k.

The interaction of schema value and participant-P(yes) was associated with activity in the pregenual ACC and medial OFC, as well as the right VLPFC and bilateral supramarginal gyri (Figure 8a). The interaction of experienced value and participant P(yes) was also associated with activity in medial OFC and a large area of the medial superior frontal gyrus and left angular gyrus (Figure 8b). There were no clusters that passed the whole-brain FWE cluster-corrected threshold for the interaction of unfamiliarity and participant-P(yes). However, given the challenge of detecting cluster corrected effects in deep brain structures, we applied a small volume correction using the striatum ROI. This analysis found that two clusters in the bilateral caudate nucleus responded to the interaction of unfamiliarity with participant-P(yes) (Figure 8c; FWE-corrected *P*'s ≤ 0.03, MNI: 18, 20, -4; -8, 22, 0). Whole brain peak activations for this GLM are described in Table 4.

Table 4. fMRI activations for model-based values GLM, including those from Figure 8

Region (AAL2)	MNI Coordinates			Number of voxels	Peak *t*-value
	x	y	z		
Unfamiliarity (k = 164)					
Left fusiform gyrus	-36	-44	-20	5360	11.10
Left inferior occipital gyrus	-28	-84	-10		8.81
Left parahippocampal gyrus	-28	-26	-24		7.25
Right fusiform gyrus	36	-56	-12	4216	11.08
Right lingual gyrus	24	-88	-6		9.38
Right fusiform gyrus	32	-38	-22		7.73
Left inferior frontal gyrus, orbitalis	-40	30	-12	3795	10.97
Left inferior frontal gyrus, opercularis	-40	4	28		9.16
Left inferior frontal gyrus, triangularis	-42	24	14		8.56
Left supplementary motor area	-8	24	48	2195	9.29
Left superior frontal gyrus, medial	-8	52	44		7.15
Left superior frontal gyrus, medial	-6	50	24		5.37
Right anterior orbital gyrus	38	40	-18	196	7.37
Left middle occipital gyrus	-24	-66	36	625	6.79
Left gyrus rectus	-4	48	-18	465	6.61
Right gyrus rectus	2	28	-20		3.94

Confidence (k = 177)					
Left superior frontal gyrus, medial	-6	50	46	302	6.00
Left cuneus	-6	-96	20	1136	5.03
Schema value x participant-P(yes) (k = 175)					
Right Rolandic operculum	52	-24	20	581	6.83
Right supramarginal gyrus	64	-28	38	581	4.27
Right superior temporal gyrus	68	-12	8	581	4.15
Right hippocampus	38	-18	-22	266	6.69
Right inferior temporal gyrus	54	-12	-36	266	3.79
Right inferior frontal gyrus, triangularis	54	34	10	383	6.48
Left paracentral lobule	-16	-12	66	176	6.42
Right middle temporal gyrus	66	-52	-2	616	6.06
Left superior temporal gyrus	-64	-30	20	483	5.88
Left postcentral gyrus	-40	-36	64	593	5.69
Left postcentral gyrus	-20	-36	74	593	5.22
Left paracentral lobule	-6	-18	68	593	3.60
Right gyrus rectus	8	44	-22	330	5.37
Right anterior cingulate	4	38	-2	330	4.42
Left lingual gyrus	-8	-68	-4	196	4.75
Right postcentral gyrus	30	-40	64	282	4.72
Left superior temporal gyrus	-60	2	-12	212	4.42
Right lingual gyrus	8	-60	4	221	4.39
Right calcarine fissure	16	-78	10	221	3.84
Experienced value x participant-P(yes) (k = 194)					
Left superior frontal gyrus, medial	-4	60	12	1439	6.92
Right superior frontal gyrus, medial	14	52	18	1439	5.08
Left gyrus rectus	-8	38	-16	1439	4.88
Left middle occipital gyrus	-34	-86	36	477	4.57
Left superior frontal gyrus	-20	32	36	201	5.01

All reported clusters were significant at the $P < 0.05$, FWE-corrected threshold at the cluster level after peak thresholding at $P < 0.001$. The critical cluster extent threshold for each contrast is given by the value of k.

We next specifically compared how activity related to participant-P(yes) in vmPFC and striatum, the two regions we identified *a priori* as being associated with valuation, was modulated by experienced value, schema value and unfamiliarity. We extracted the mean

933 beta coefficients for the interaction between participant-P(yes) and these three terms in the
934 vmPFC and striatum ROIs. The interaction of participant-P(yes) with experienced and
935 schema value was significant in vmPFC (one-tailed, one sample t-tests against zero: t's(22) ≥
936 2.99, $P \leq 0.003$, d's ≥ 0.62), but not the striatum ($t(22) \leq 1.25$, $P \geq 0.1$, d's ≤ 0.26), whereas
937 the interaction of participant-P(yes) with unfamiliarity was significant in the striatum ($t(22)$
938 $= 2.65$, $P = 0.007$, $d = 0.55$), but not vmPFC ($t(22) = 1.30$, $P = 0.1$, $d = 0.27$). Thus, vmPFC
939 responded to greater agreement between both experienced and schema values with
940 participant-P(yes), while striatum activity increased in response to participant-P(yes) when
941 unfamiliarity was high.

942 To examine whether ROIs differed in their response to these value-related terms, we
943 then tested an ROI (striatum, vmPFC) by modulator (interactions of participant-P(yes) with
944 experienced value, schema value and unfamiliarity) interaction on these average beta
945 coefficients (Figure 9). This interaction was highly significant ($F_{2,44} = 12.01$, $P < 0.0001$, $\eta_p^2 =$
946 0.35), as was a main effect of ROI ($F_{1,22} = 14.09$, $P < 0.01$, $\eta_p^2 = 0.39$), but not modulator ($F_{2,44}$
947 $= 0.25$, $P = 0.8$, $\eta_p^2 = 0.01$). To determine the source of this interaction, we compared the
948 difference of the betas in the vmPFC and striatum for each modulator (i.e. the effect of each
949 interaction between ROIs). This difference was significantly greater for the interaction of
950 participant-P(yes) with experienced value compared to both schema value and unfamiliarity
951 (Bonferroni corrected t-tests t's(22) ≥ 3.75, P's < 0.01, $d \geq 0.78$), but there was no comparable
952 significant difference between schema value and unfamiliarity.

953 To summarize, vmPFC activity reflected the influence of experienced and schema
954 values on participants' value judgments, and preferentially reflected the influence of
955 explicitly experienced values on participants' value judgments compared to the striatum.

Striatal activity reflected the effect of unfamiliarity on participants' value judgments, but not value information stored directly in memory or inferred from schematic associations.

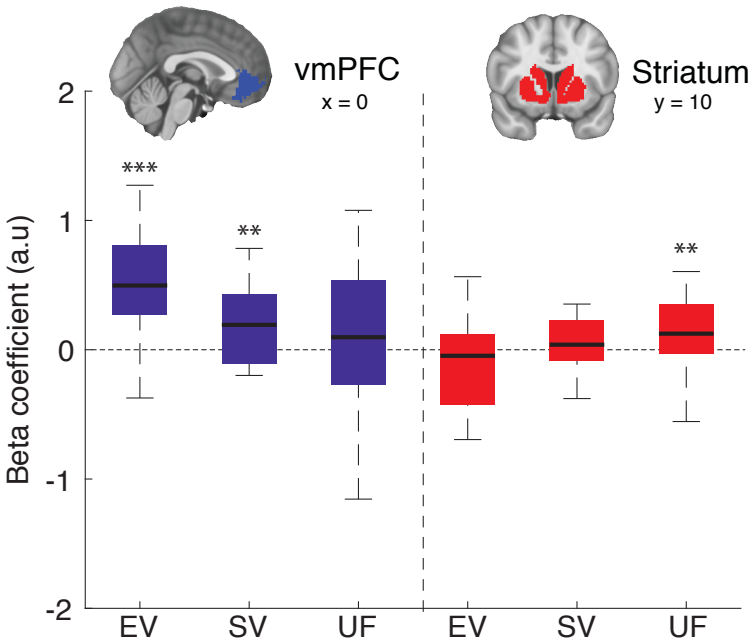

Figure 9. Boxplots showing mean beta coefficients from voxels in ventromedial prefrontal cortex (vmPFC) and striatum ROIs for interactions of participant-P(yes) with experienced value (EV), schema value (SV) and unfamiliarity (UF). *** $P < 0.001$, ** $P < 0.01$, one-tailed one-sample t-test against zero.

Generalized psychophysical interactions

We hypothesized that differential demand on memory systems during decision-making would also lead to distinct patterns of functional connectivity, reflecting the contributions of different memory stores to the assessment of options. vmPFC has reciprocal connections with regions of middle temporal cortex (MTC) and anterior ventrolateral prefrontal cortex (aVLPFC) (Price, 2007; Saleem, Kondo, & Price, 2008). Both vmPFC and striatum also receive input from the hippocampus (HPC). We were principally interested in whether vmPFC and MTC connectivity increased with greater demands on schema-based decision-making, and whether striatum and HPC connectivity increased during the assessment of directly experienced values. To address this hypothesis, we carried out

968 generalized psychophysical interaction (gPPI) analyses that contrasted how connectivity
969 between pairs of ROIs listed in Table 1 changed between task conditions, as well as more
970 exploratory seed-to-voxel whole-brain gPPI analyses focused on vmPFC, MTC, HPC and
971 striatum.

972 We first examined whether connectivity with vmPFC and MTC was modulated by
973 demands on schematic knowledge about ingredients and their value on correct responses in
974 the first presentation. Within an MTC seed, there was increased connectivity with vmPFC on
975 the first presentation of positive recipe ingredients compared to negative recipe ingredients
976 (Bonferroni corrected t-test: $t(21) = 4.00$, $P < 0.01$, $d = 0.85$), but not any other ROI ($P \geq 0.2$,
977 Bonferroni corrected). Similarly, using vmPFC as a seed ROI revealed increased connectivity
978 with the MTC ROI in the same contrast (Bonferroni corrected t-test: $t(21) = 3.68$, $P < 0.05$, d
979 $= 0.78$), but not any other ROI. An exploratory whole-brain seed-to-voxel analysis on this
980 contrast with the MTC ROI as a seed found that this region had significantly greater
981 connectivity with a cluster on the medial frontal wall overlapping with our vmPFC ROI
982 (Figure 10a, MNI: -2, 46, -12), and a second cluster in lateral occipital cortex (MNI: -52, -68,
983 12). The same whole-brain ROI-to-voxel contrast with the vmPFC ROI as a seed did not reveal
984 any significant clusters at an FWE cluster-corrected threshold.

985 These data provide evidence that vmPFC and MTC connectivity changed depending
986 on the value of recipe ingredients on the first presentation. To examine whether this effect
987 might depend on successful retrieval of relevant schema-value information, we tested the
988 interaction of value and accuracy on the first presentation of recipe ingredients. This
989 interaction was significant when either vmPFC and MTC was used as a seed (Bonferroni
990 corrected t-tests: t's$(20) \geq 2.95$, $P < 0.05$, $d \geq 0.64$), but not between these seeds and any

991 other ROIs. There was no main effect of accuracy on connectivity between ROIs on these
992 trials. We further examined whether this value related increase in vmPFC-MTC connectivity
993 was higher on the first presentation than subsequent presentations by testing the interaction
994 of presentation number and value for recipe ingredients, but this interaction did not reach
995 significance after correction for multiple comparisons in either seed.

996 Thus, vmPFC-MTC connectivity increased in response to retrieval of positive values
997 inferred from schematic knowledge on this first presentation, and though this increase was
998 greater on correct trials compared to errors, there were no main effects of clustering
999 condition or accuracy. These null effects could partially stem from participants attempting
1000 to retrieve schematic associations on the first presentation in all conditions, consistent with
1001 greater MTC activity in these presentations compared to repetitions in the independent
1002 condition.

1003 We also tested whether connectivity between MTC and vmPFC and any other ROIs
1004 depended on clustering status by contrasting the recipe and independent conditions on the
1005 first presentation, collapsing across value. There was no significant change in connectivity
1006 between MTC, vmPFC and any other ROIs in this contrast. Exploratory seed-to-voxel
1007 analyses for both of these contrasts were similarly null.

1008 Next, we investigated if connectivity between with the HPC and striatum and other
1009 ROIs depended on the value of options in the second and third presentations. Contrasting
1010 positive and negative independent ingredients in these trials, we did not find any significant
1011 increase in connectivity between HPC and striatum with each other or any other region in
1012 ROI-to-ROI, or seed-to-voxel analyses. We further examined if connectivity with these ROIs
1013 was higher for positive than negative ingredients in the independent condition relative to

the recipe condition by testing the interaction of value and clustering. This analysis was similarly null for both seeds.

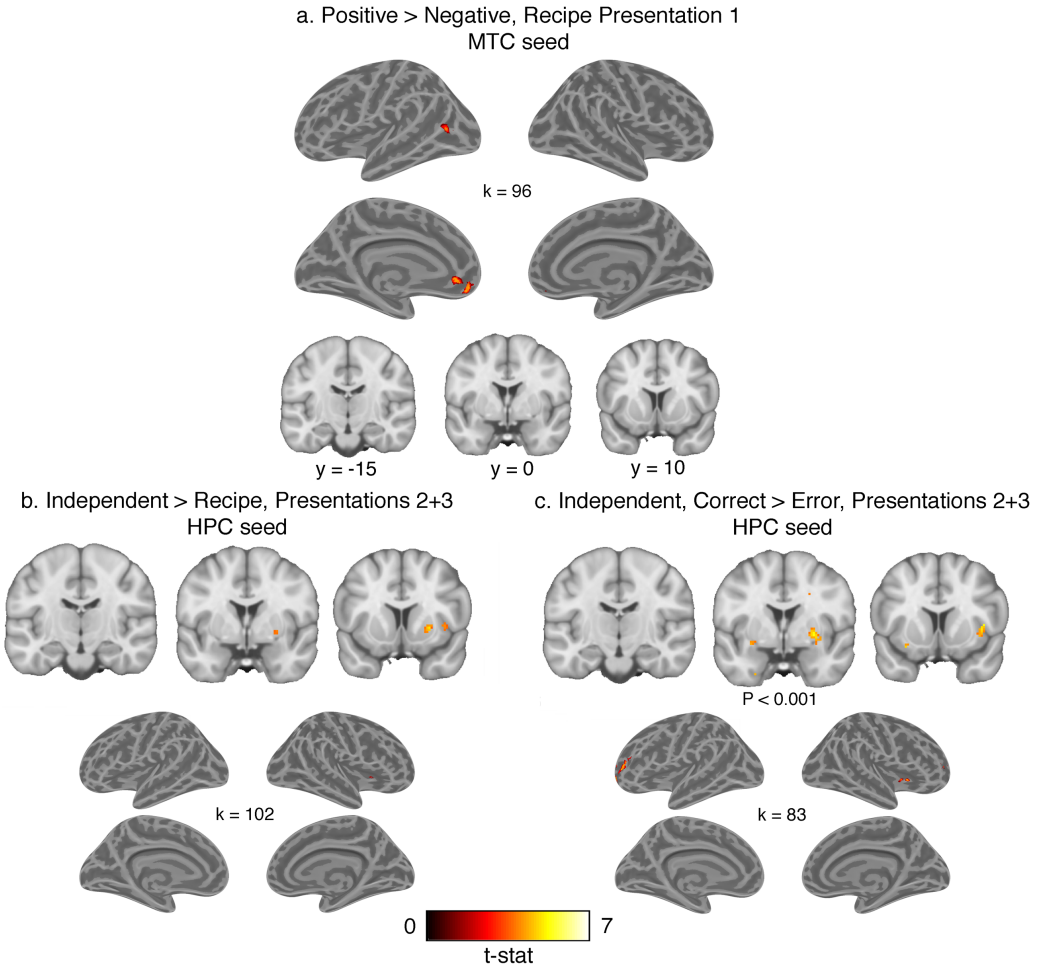

Figure 10. Whole brain t-statistic maps for seed-to-voxel generalized psychophysical interaction analyses. **a.** Voxels with increased connectivity with the middle temporal cortex (MTC) seed on the first presentation of positive recipe trials compared to negative recipe trials. **b.** Voxels with greater connectivity with the hippocampus (HPC) seed on the second and third presentation of independent trials compared to recipe trials. **c.** Voxels with increased connectivity with HPC on correct compared to error trials on the second and third presentations of independent ingredients. Voxels passing the P <0.05 FWE cluster corrected threshold are shown in all panels except for top row of **c.** Cluster extent threshold is given by k.

We also tested if HPC and striatum connectivity depended on demands for retrieving previously experienced feedback associated with particular ingredient instance. Collapsing

across value conditions, we contrasted independent and recipe ingredients on the second and third presentations where ingredient values could be retrieved from episodic memory, with the expectation that demand on episodic memory would be greater in the independent condition. There was no significant difference in connectivity between the striatum or HPC with any other ROIs in this contrast. However, a seed-to-voxel whole-brain analysis with the HPC seed showed significantly greater connectivity with a cluster in the right putamen and insula (Figure 10b; MNI: 26, 10, 0). The reverse seed-to-voxel analysis with the striatum ROI as a seed did not reveal significant clusters within a small-volume corrected HPC ROI.

To test if this increase in HPC and hippocampus connectivity was related to retrieval success we also contrasted correct and error responses on the second and third presentation of independent ingredients. Using the HPC as a seed in a seed-to-voxel analysis, we found increased connectivity with this ROI and the right putamen (MNI: 28, 2, 4) after small volume correction within the striatum ROI. An exploratory whole-brain analysis also found that HPC significantly increased connectivity with clusters in bilateral anterior rostrolateral PFC and right insula (Figure 10c). However, there were no significant differences in connectivity between these conditions in ROI-to-ROI contrasts with either HPC or striatum as seeds. The reverse ROI-to-voxel analysis with the striatum ROI as a seed did not reveal significant increase in connectivity in a small-volume corrected HPC ROI. All peaks from seed-to-voxel analyses are reported in Table 5.

1042 **Table 5. Whole brain seed-to-voxel connectivity effects from Figure 10**

Region (AAL2)	MNI Coordinates			Number of voxels	Peak *t*-value
	x	y	z		
Recipe Positive > Recipe negative, presentation 1, correct — MTC seed (k = 96)					
Left superior frontal gyrus, medial orbital	-2	46	-12	351	6.42
Left middle temporal gyrus	-52	-68	12	112	5.30
Correct > Error, independent presentations 2 and 3, correct — HPC seed (k = 83)					
Left middle frontal gyrus	-40	52	20	253	6.14
Left superior frontal gyrus, dorsolateral	-18	54	-4	253	5.66
Right insula	36	18	0	100	5.76
Right superior frontal gyrus, dorsolateral	30	54	14	122	5.76

1043 All reported clusters were significant at the $P < 0.05$, FWE-corrected threshold at the
1044 cluster level after peak thresholding at $P < 0.001$. The critical cluster extent threshold for
1045 each contrast is given by the value of k.
1046
1047 In summary, we found that vmPFC-MTC connectivity depended on recipe value
1048 associations on the first presentation where this information was key to guiding choice.
1049 Meanwhile, HPC increased connectivity with the right putamen in response to greater
1050 demand on episodic memory compared to trials where schema memory could still be used,
1051 and trials where value information was not successfully retrieved.

1052 **Discussion**

1053 Here we investigated the neural circuitry involved in value judgments based on
1054 distinct memory sources. Functional neuroimaging results implicated the vmPFC in
1055 representing both experienced and inferred values, while striatal activity correlated with the
1056 influence of unsigned memory strength on value judgment. Thus, these regions play separate
1057 roles in memory-based value judgment and decision-making.

Participants were able to infer the value of ingredients based on schematic knowledge without feedback, and continued showing a benefit from recipe information in subsequent presentations. Our computational model captured this behavior using normative information about ingredient-recipe associations. Notably, freely fitting the number of dimensions used in reconstructing these recipe-ingredient associations substantially improved the fit of the model, implying that participants varied in the depth of semantic knowledge they employed in this task. The positive recipe also had a greater influence on behavior compared to the negative recipe, indicating that participants prioritized searching associations with this recipe first — possibly because they adopted a default response to pass on ingredients where they could not retrieve positive value information.

Memory strength, expressed as unfamiliarity, also had a substantial impact on participants' willingness to endorse ingredients. Participants demonstrated a general tendency against betting on independent ingredients on the first presentation. Given that there was an equal proportion of positive and negative value ingredients, and a 2:1 ratio of points gained to lost on a bet, this behavior reflects a deviation from a rational maximization of expected value, akin to loss aversion (Kahneman & Tversky, 1979). Whereas uncertainty is often operationalized as descriptive or experienced probabilities of outcomes in behavioral economics, here it depended on the strength of participants' memory of outcomes. These results are also consistent with work showing a bias toward remembered items in preference-based choice (Gluth, Sommer, Rieskamp, & Buchel, 2015). In real terms, people appear to apply a meta-cognitive strategy where the strength of evidence from memory affects option value, regardless of its content. We would thus predict that a strong

memory for a weakly positive or negative value would be more likely to drive a response than a weak memory for a strongly positive or negative value.

Our results indicate that vmPFC represents values based on multiple memory sources. These findings add to past work demonstrating that the value function represented in vmPFC can flexibly bend to accommodate attentional priority toward different option attributes (Hare, Malmaud, & Rangel, 2011; Hunt, Dolan, & Behrens, 2014; Leong, Radulescu, Daniel, DeWoskin, & Niv, 2017; Rudorf & Hare, 2014).

We had predicted that vmPFC would be engaged more by schema-based value inference that retrieval of a specific experience. This prediction was based on lesion evidence demonstrating that vmPFC is not necessary for value judgment *per se* (Reber et al., 2017; Vaidya & Fellows, 2015; Yu, Dana, & Kable, 2018), but is needed for incorporating higher-order information into value judgments (Vaidya, Sefranek, & Fellows, 2017; Xia, Stolle, Gidengil, & Fellows, 2015). Other work has shown that inactivation or damage to vmPFC or OFC does not affect decision-making or value judgment in situations where values can be retrieved from prior direct experience, but does so when this information must be inferred from structured knowledge about a task (Bradfield et al., 2015; Izquierdo et al., 2004; Jones et al., 2012; Rudebeck, Saunders, Prescott, Chau, & Murray, 2013).

There may be a few factors contributing to this discrepancy. While experienced values were learned over many repeated exposures in these lesion experiments, here they were learned from just one or two trials. Recent work has shown that spaced, brief training over a period of days in a reinforcement learning task increases fMRI value signals in vmPFC compared to an equivalent number of trials within a single session (Wimmer, Li, Gorgolewski, & Poldrack, 2018), implying that this region is engaged more when value

judgments rely on episodic memory rather than massed experience. Although our results suggest the involvement of vmPFC in representing both directly experienced and schema-based values, this information may be robustly represented by other regions that do not depend on vmPFC to influence behavior. Studying the effects of vmPFC damage in this task could help assess when this region is critical for memory-based value judgment.

Our hypotheses are not fully committed to the precise format of experienced values in this task. Our design required that participants store information about feedback paired with ingredients in a small number of trials as a specific experience separated by other trials over a long interval. We assumed that participants would mostly rely on episodic memory for robust retention of such information. However, we cannot rule out the possibility that value information would also be stored in other ways (e.g. in working memory, or through conditioned stimulus-response mappings). Nonetheless, this possibility does not change our ability to contrast inference of values from a memory schema and reliance on direct experience more generally.

Notably, our results indicate that interactions between vmPFC and MTC support inference of values from semantic knowledge. Other work has shown that utilization of semantic meaning in value judgments increases interactions between vmPFC and regions of left middle and superior temporal cortex (Lim, O'Doherty, & Rangel, 2013). Here, vmPFC-MTC connectivity depended on the value of schematic associations. This result could reflect the accumulation of value information through the interaction between these regions, or the differential weight given to positive and negative recipes, as there was behavioral evidence that participants prioritized positive recipe associations. In either case, these data provide evidence that engagement between vmPFC and semantic memory stores is involved in

inferential value judgments based on real-world structured knowledge in absence of explicit experience values.

This experiment explicitly crossed two features commonly associated with the vmPFC, but rarely compared within the same task: value coding and schema-based memory and inference (Chan, Niv, & Norman, 2016; Delgado et al., 2016; Ghosh, Moscovitch, Melo Colella, & Gilboa, 2014). Our data are consistent both proposed roles for this region: with schema-related knowledge playing a role in value construction in vmPFC, and with this region responding to utilization of schema-related knowledge more generally. Recent rodent electrophysiological data also indicate that value and schematic task representations co-exist in separable codes within OFC (Zhou et al., 2019), suggesting these functions may co-exist within the same regions.

The role of striatum in memory tasks has been the focus of recent research, with several hypotheses being considered (Elward et al., 2015; King, Chastelaine, Elward, Wang, & Rugg, 2018; Schwarze, Bingel, Badre, & Sommer, 2013; Scimeca & Badre, 2012). Here, activity in the striatum integrated the influence of memory strength on participants' decisions to bet or pass on ingredients, as its activity correlated with the interaction of participant-P(yes) and unfamiliarity. Relatedly, recent work from our group has observed that the striatum tracked prediction errors for retrieval success during a recognition memory task (Scimeca et al., 2016), analogous to its role in action selection and reinforcement-learning (Garrison, Erdeniz, & Done, 2013; Haber & Knutson, 2010; Pessiglione, Seymour, Flandin, Dolan, & Frith, 2006). These prediction errors were correlated with changes in the criterion by which evidence from memory was evaluated. Unlike conventional reinforcement learning settings, the striatum was sensitive to

prediction errors that derived from memory strength rather than the value of a response. We expand on those findings here, demonstrating that the striatum responds to the influence of memory strength on participants' willingness to make a bet in a value-based decision-making task, independent of memory valence. Together, these results imply a role for the striatum in a cognitive decision about when to act based on memory strength, equivalent to its role in controlling a tendency to bet in risky decision-making (Knutson, Wimmer, Kuhnen, & Winkielman, 2008; Nachev et al., 2015; Zalocusky et al., 2016), or in gating working memory (Chatham & Badre, 2015).

Notably, the striatum responded to the strength of memory for experienced values rather than the values of options themselves. The striatum responds to successful memory retrieval (Spaniol et al., 2009), though the functional significance of this activation is debated. Some work has argued that these signals reflect a value signal that depends on the congruence of the memory task with participants' goals (Han et al., 2010), while others have suggested that striatal reward and retrieval signals are distinct (Elward et al., 2015). Here we found evidence that unsigned memory strength modulates striatal value signals, but the signed experienced value of options did not. These data indicate that value and retrieval signals in the striatum may follow a common dimension that corresponds to the utility of retrieved information given task demands — biasing cortical representations of associated actions based on the strength of information recovered from retrieval.

We also observed that connectivity between HPC and the striatum increased in the second and third presentations of independent ingredients compared to recipe ingredients, and on correct choices for independent ingredients compared to error trials. This result implies that HPC-striatal communication is involved in successful retrieval of experienced

ingredient-value associations. While this result depended on the choice of seed ROI, this apparent selectivity might owe to our striatal ROI averaging over functionally distinct subregions.

In conclusion, we demonstrated the involvement of the striatum and vmPFC in distinct processes within memory-based decision-making. Our data provide fresh insights into the dynamics of this circuitry, with a view into the intersection of decision-making and memory that is the seat of much real-world choice behavior. These results have implications for understanding the origins of decision-making impairments in neurodegenerative diseases such as Alzheimer's disease and frontotemporal dementia (Salmon & Bondi, 2009), as well as Parkinson's disease (Edelstyn, Shepherd, Mayes, Sherman, & Ellis, 2010). New insights into the interaction of these circuits may have relevance for clinical interventions or treatments.

References

Badre, D., Poldrack, R. A., Pare-Blagoev, E. J., Insler, R. Z., & Wagner, A. D. (2005a). Dissociable controlled retrieval and generalized selection mechanisms in ventrolateral prefrontal cortex. *Neuron, 47*(6), 907-918. doi:10.1016/j.neuron.2005.07.023

Badre, D., Poldrack, R. A., Pare-Blagoev, E. J., Insler, R. Z., & Wagner, A. D. (2005b). Dissociable controlled retrieval and generalized selection mechanisms in ventrolateral prefrontal cortex. *Neuron, 47*(6), 907-918. doi:10.1016/j.neuron.2005.07.023

Barron, H. C., Dolan, R. J., & Behrens, T. E. (2013). Online evaluation of novel choices by simultaneous representation of multiple memories. *Nat Neurosci, 16*(10), 1492-1498. doi:10.1038/nn.3515

Bartlett, F. C. (1932). *Remembering: A Study in Experimental and Social Psychology*: Cambridge University Press.

Bartra, O., McGuire, J. T., & Kable, J. W. (2013). The valuation system: a coordinate-based meta-analysis of BOLD fMRI experiments examining neural correlates of subjective value. *Neuroimage, 76*, 412-427. doi:10.1016/j.neuroimage.2013.02.063

Blechert, J., Meule, A., Busch, N. A., & Ohla, K. (2014). Food-pics: an image database for experimental research on eating and appetite. *Front Psychol, 5*, 617. doi:10.3389/fpsyg.2014.00617

Bradfield, L. A., Dezfouli, A., van Holstein, M., Chieng, B., & Balleine, B. W. (2015). Medial Orbitofrontal Cortex Mediates Outcome Retrieval in Partially Observable Task Situations. *Neuron, 88*(6), 1268-1280. doi:10.1016/j.neuron.2015.10.044

Braga, R. M., & Buckner, R. L. (2017). Parallel Interdigitated Distributed Networks within the Individual Estimated by Intrinsic Functional Connectivity. *Neuron, 95*(2), 457-471 e455. doi:10.1016/j.neuron.2017.06.038

Brainard, D. H. (1997). The psychophysics toolbox. *Spatial Vision, 10*(4), 433-436. doi:Doi 10.1163/156856897x00357

Brett, M., Anton, J., Valabregue, R., & Poline, J. (2002). *Region of interest analysis using an SPM toolbox*. Paper presented at the 8th International Conference on Functional Mapping of the Human Brain, Sendai, Japan.

Brodeur, M. B., Dionne-Dostie, E., Montreuil, T., & Lepage, M. (2010). The Bank of Standardized Stimuli (BOSS), a new set of 480 normative photos of objects to be used as visual stimuli in cognitive research. *PLoS One, 5*(5), e10773. doi:10.1371/journal.pone.0010773

Brodeur, M. B., Guerard, K., & Bouras, M. (2014). Bank of Standardized Stimuli (BOSS) phase II: 930 new normative photos. *PLoS One, 9*(9), e106953. doi:10.1371/journal.pone.0106953

Chan, S. C. Y., Niv, Y., & Norman, K. A. (2016). A Probability Distribution over Latent Causes, in the Orbitofrontal Cortex. *Journal of Neuroscience, 36*(30), 7817-7828. doi:10.1523/JNEUROSCI.0659-16.2016

Chatham, C. H., & Badre, D. (2015). Multiple gates on working memory. *Curr Opin Behav Sci, 1*, 23-31. doi:10.1016/j.cobeha.2014.08.001

Delgado, M. R., Beer, J. S., Fellows, L. K., Huettel, S. A., Platt, M. L., Quirk, G. J., & Schiller, D. (2016). Viewpoints: Dialogues on the functional role of the ventromedial prefrontal cortex. *Nat Neurosci, 19*(12), 1545-1552. doi:10.1038/nn.4438

Dumais, S. T. (2004). Latent semantic analysis. *Annual Review of Information Science and Technology, 38*, 189-230.

Edelstyn, N. M., Shepherd, T. A., Mayes, A. R., Sherman, S. M., & Ellis, S. J. (2010). Effect of disease severity and dopaminergic medication on recollection and familiarity in patients with idiopathic nondementing Parkinson's. *Neuropsychologia, 48*(5), 1367-1375. doi:10.1016/j.neuropsychologia.2009.12.039

Eichenbaum, H. (2017). Memory: Organization and Control. *Annu Rev Psychol, 68*, 19-45. doi:10.1146/annurev-psych-010416-044131

Elward, R. L., Vilberg, K. L., & Rugg, M. D. (2015). Motivated Memories: Effects of Reward and Recollection in the Core Recollection Network and Beyond. *Cereb Cortex, 25*(9), 3159-3166. doi:10.1093/cercor/bhu109

Garrison, J., Erdeniz, B., & Done, J. (2013). Prediction error in reinforcement learning: a meta-analysis of neuroimaging studies. *Neurosci Biobehav Rev, 37*(7), 1297-1310. doi:10.1016/j.neubiorev.2013.03.023

Ghosh, V. E., & Gilboa, A. (2014). What is a memory schema? A historical perspective on current neuroscience literature. *Neuropsychologia, 53*, 104-114. doi:10.1016/j.neuropsychologia.2013.11.010

Ghosh, V. E., Moscovitch, M., Melo Colella, B., & Gilboa, A. (2014). Schema representation in patients with ventromedial PFC lesions. *J Neurosci, 34*(36), 12057-12070. doi:10.1523/JNEUROSCI.0740-14.2014

Gluth, S., Sommer, T., Rieskamp, J., & Buchel, C. (2015). Effective Connectivity between Hippocampus and Ventromedial Prefrontal Cortex Controls Preferential Choices from Memory. *Neuron, 86*(4), 1078-1090. doi:10.1016/j.neuron.2015.04.023

Haber, S. N., & Knutson, B. (2010). The reward circuit: linking primate anatomy and human imaging. *Neuropsychopharmacology, 35*(1), 4-26. doi:10.1038/npp.2009.129

Han, S., Huettel, S. A., Raposo, A., Adcock, R. A., & Dobbins, I. G. (2010). Functional Significance of Striatal Responses during Episodic Decisions: Recovery or Goal Attainment? *Journal of Neuroscience, 30*(13), 4767-4775. doi:10.1523/Jneurosci.3077-09.2010

Hare, T. A., Malmaud, J., & Rangel, A. (2011). Focusing attention on the health aspects of foods changes value signals in vmPFC and improves dietary choice. *J Neurosci, 31*(30), 11077-11087. doi:10.1523/JNEUROSCI.6383-10.2011

Hunt, L. T., Dolan, R. J., & Behrens, T. E. (2014). Hierarchical competitions subserving multi-attribute choice. *Nat Neurosci, 17*(11), 1613-1622. doi:10.1038/nn.3836

Izquierdo, A., Suda, R. K., & Murray, E. A. (2004). Bilateral orbital prefrontal cortex lesions in rhesus monkeys disrupt choices guided by both reward value and reward contingency. *J Neurosci, 24*(34), 7540-7548. doi:10.1523/JNEUROSCI.1921-04.2004

Jones, J. L., Esber, G. R., McDannald, M. A., Gruber, A. J., Hernandez, A., Mirenzi, A., & Schoenbaum, G. (2012). Orbitofrontal Cortex Supports Behavior and Learning Using Inferred But Not Cached Values. *Science, 338*(6109), 953-956. doi:Doi 10.1126/Science.1227489

Kahneman, D., & Tversky, A. (1979). Prospect Theory - Analysis of Decision under Risk. *Econometrica, 47*(2), 263-291. doi:Doi 10.2307/1914185

King, D. R., Chastelaine, M., Elward, R. L., Wang, T. H., & Rugg, M. D. (2018). Dissociation between the neural correlates of recollection and familiarity in the striatum and hippocampus: Across-study convergence. *Behav Brain Res, 354*, 1-7. doi:10.1016/j.bbr.2017.07.031

Kleiner, M., Brainard, D., & Pelli, D. (2007). What's new in Psychtoolbox-3? *Perception, 36*, 14-14.

Knutson, B., Wimmer, G. E., Kuhnen, C. M., & Winkielman, P. (2008). Nucleus accumbens activation mediates the influence of reward cues on financial risk taking. *Neuroreport, 19*(5), 509-513. doi:10.1097/WNR.0b013e3282f85c01

Landauer, T. K., Foltz, P. W., & Laham, D. (1998). An introduction to latent semantic analysis. *Discourse Processes, 25*(2-3), 259-284. doi:Doi 10.1080/01638539809545028

Leong, Y. C., Radulescu, A., Daniel, R., DeWoskin, V., & Niv, Y. (2017). Dynamic Interaction between Reinforcement Learning and Attention in Multidimensional Environments. *Neuron, 93*(2), 451-463. doi:10.1016/j.neuron.2016.12.040

Lim, S. L., O'Doherty, J. P., & Rangel, A. (2013). Stimulus value signals in ventromedial PFC reflect the integration of attribute value signals computed in fusiform gyrus and posterior superior temporal gyrus. *J Neurosci, 33*(20), 8729-8741. doi:10.1523/JNEUROSCI.4809-12.2013

Nachev, P., Lopez-Sosa, F., Gonzalez-Rosa, J. J., Galarza, A., Avecillas, J., Pineda-Pardo, J. A., . . . Strange, B. (2015). Dynamic risk control by human nucleus accumbens. *Brain, 138*, 3496-3502. doi:10.1093/brain/awv285

Pessiglione, M., Seymour, B., Flandin, G., Dolan, R. J., & Frith, C. D. (2006). Dopamine-dependent prediction errors underpin reward-seeking behaviour in humans. *Nature, 442*(7106), 1042-1045. doi:10.1038/nature05051

Piaget, J. (1952). *The Origins of Intelligence in Children* (Vol. 8). International Universities Press.

Postman, L., & Keppel, G. (1970). *Norms of Word Asociation*. New York, New York: Academic Press.

Price, J. L. (2007). Definition of the orbital cortex in relation to specific connections with limbic and visceral structures and other cortical regions. *Ann N Y Acad Sci, 1121*, 54-71. doi:annals.1401.008 [pii]
10.1196/annals.1401.008

Ratcliff, R. (1978). Theory of Memory Retrieval. *Psychological Review, 85*(2), 59-108. doi:Doi 10.1037//0033-295x.85.2.59

Reber, J., Feinstein, J. S., O'Doherty, J. P., Liljeholm, M., Adolphs, R., & Tranel, D. (2017). Selective impairment of goal-directed decision-making following lesions to the human ventromedial prefrontal cortex. *Brain, 140*(6), 1743-1756. doi:10.1093/brain/awx105

Rescorla, R. A., & Wagner, A. R. (1972). A theory of Pavlovian conditioning: Variations in the effective- ness of reinforcement and non-reinforcement. In A. H. Black & W. F. Prokasy (Eds.), *Classical conditioning. II. Current research and theory* (pp. 64-99). New York: Appleton-Century-Crofts.

Roy, M., Shohamy, D., & Wager, T. D. (2012). Ventromedial prefrontal-subcortical systems and the generation of affective meaning. *Trends Cogn Sci, 16*(3), 147-156. doi:10.1016/j.tics.2012.01.005

Rudebeck, P. H., Saunders, R. C., Prescott, A. T., Chau, L. S., & Murray, E. A. (2013). Prefrontal mechanisms of behavioral flexibility, emotion regulation and value updating. *Nat Neurosci, 16*(8), 1140-1145. doi:10.1038/nn.3440

Rudorf, S., & Hare, T. A. (2014). Interactions between Dorsolateral and Ventromedial Prefrontal Cortex Underlie Context-Dependent Stimulus Valuation in Goal-Directed Choice. *Journal of Neuroscience, 34*(48), 15988-15996. doi:10.1523/JNEUROSCI.3192-14.2014

Saleem, K. S., Kondo, H., & Price, J. L. (2008). Complementary circuits connecting the orbital and medial prefrontal networks with the temporal, insular, and opercular cortex in the macaque monkey. *J Comp Neurol, 506*(4), 659-693. doi:10.1002/cne.21577

Salmon, D. P., & Bondi, M. W. (2009). Neuropsychological assessment of dementia. *Annu Rev Psychol, 60*, 257-282. doi:10.1146/annurev.psych.57.102904.190024

Schuck, N. W., Cai, M. B., Wilson, R. C., & Niv, Y. (2016). Human Orbitofrontal Cortex Represents a Cognitive Map of State Space. *Neuron, 91*(6), 1402-1412. doi:10.1016/j.neuron.2016.08.019

Schwarze, U., Bingel, U., Badre, D., & Sommer, T. (2013). Ventral striatal activity correlates with memory confidence for old- and new-responses in a difficult recognition test. *PLoS One, 8*(3), e54324. doi:10.1371/journal.pone.0054324

Scimeca, J. M., & Badre, D. (2012). Striatal contributions to declarative memory retrieval. *Neuron, 75*(3), 380-392. doi:10.1016/j.neuron.2012.07.014

Scimeca, J. M., Katzman, P. L., & Badre, D. (2016). Striatal prediction errors support dynamic control of declarative memory decisions. *Nat Commun, 7*, 13061. doi:10.1038/ncomms13061

Shadlen, M. N., & Shohamy, D. (2016). Decision Making and Sequential Sampling from Memory. *Neuron, 90*(5), 927-939. doi:10.1016/j.neuron.2016.04.036

Spaniol, J., Davidson, P. S., Kim, A. S., Han, H., Moscovitch, M., & Grady, C. L. (2009). Event-related fMRI studies of episodic encoding and retrieval: meta-analyses using activation likelihood estimation. *Neuropsychologia, 47*(8-9), 1765-1779. doi:10.1016/j.neuropsychologia.2009.02.028

Thompson-Schill, S. L., D'Esposito, M., Aguirre, G. K., & Farah, M. J. (1997). Role of left inferior prefrontal cortex in retrieval of semantic knowledge: a reevaluation. *Proc Natl Acad Sci U S A, 94*(26), 14792-14797.

Tzourio-Mazoyer, N., Landeau, B., Papathanassiou, D., Crivello, F., Etard, O., Delcroix, N., . . . Joliot, M. (2002). Automated anatomical labeling of activations in SPM using a macroscopic anatomical parcellation of the MNI MRI single-subject brain. *Neuroimage, 15*(1), 273-289. doi:10.1006/nimg.2001.0978

Vaidya, A. R., & Fellows, L. K. (2015). Testing necessary regional frontal contributions to value assessment and fixation-based updating. *Nat Commun, 6*, 10120. doi:10.1038/ncomms10120

Vaidya, A. R., Sefranek, M., & Fellows, L. K. (2017). Ventromedial Frontal Lobe Damage Alters how Specific Attributes are Weighed in Subjective Valuation. *Cereb Cortex*, 1-11. doi:10.1093/cercor/bhx246

Whitfield-Gabrieli, S., & Nieto-Castanon, A. (2012). Conn: a functional connectivity toolbox for correlated and anticorrelated brain networks. *Brain Connect, 2*(3), 125-141. doi:10.1089/brain.2012.0073

Wilson, R. C., Takahashi, Y. K., Schoenbaum, G., & Niv, Y. (2014). Orbitofrontal cortex as a cognitive map of task space. *Neuron, 81*(2), 267-279. doi:10.1016/j.neuron.2013.11.005

Wimmer, G. E., Li, J. M. K., Gorgolewski, K. J., & Poldrack, R. A. (2018). Reward Learning over Weeks Versus Minutes Increases the Neural Representation of Value in the Human Brain. *Journal of Neuroscience, 38*(35), 7649-7666. doi:10.1523/Jneurosci.0075-18.2018

Xia, C., Stolle, D., Gidengil, E., & Fellows, L. K. (2015). Lateral orbitofrontal cortex links social impressions to political choices. *J Neurosci, 35*(22), 8507-8514. doi:10.1523/JNEUROSCI.0526-15.2015

Yonelinas, A. P. (1994). Receiver-Operating Characteristics in Recognition Memory - Evidence for a Dual-Process Model. *Journal of Experimental Psychology-Learning Memory and Cognition, 20*(6), 1341-1354. doi:Doi 10.1037/0278-7393.20.6.1341

Yu, L. Q., Dana, J., & Kable, J. W. (2018). Individuals with ventromedial frontal damage have more unstable but still fundamentally transitive preferences. *bioRxiv, 384024*. doi:10.1101/384024

Zalocusky, K. A., Ramakrishnan, C., Lerner, T. N., Davidson, T. J., Knutson, B., & Deisseroth, K. (2016). Nucleus accumbens D2R cells signal prior outcomes and control risky decision-making. *Nature, 531*(7596), 642-646. doi:10.1038/nature17400

Zhou, J., Gardner, M. P. H., Stalnaker, T. A., Ramus, S. J., Wikenheiser, A. M., Niv, Y., & Schoenbaum, G. (2019). Rat Orbitofrontal Ensemble Activity Contains Multiplexed but Dissociable Representations of Value and Task Structure in an Odor Sequence Task. *Curr Biol, 29*(6), 897-907 e893. doi:10.1016/j.cub.2019.01.048